Mycobacterium tuberculosis response to cholesterol is integrated with environmental pH and potassium levels via a lipid utilization regulator

Yue Chen[1], Nathan J. MacGilvary[1], and Shumin Tan[1*]

[1]Department of Molecular Biology and Microbiology, Tufts University School of Medicine, Boston, Massachusetts 02111, USA.

*Corresponding author: shumin.tan@tufts.edu

10 **SUMMARY**

11 How bacterial response to environmental cues and nutritional sources may be integrated in
12 enabling host colonization is poorly understood. Exploiting a reporter-based screen, we discovered
13 that overexpression of *Mycobacterium tuberculosis* (Mtb) lipid utilization regulators altered Mtb
14 acidic pH response dampening by low environmental potassium (K^+). Transcriptional analyses
15 unveiled amplification of Mtb response to acidic pH in the presence of cholesterol, a major carbon
16 source for Mtb during infection, and vice versa. Strikingly, deletion of the putative lipid regulator
17 *mce3R* resulted in loss of augmentation of (i) cholesterol response at acidic pH, and (ii) low [K^+]
18 response by cholesterol, with minimal effect on Mtb response to each signal individually. Finally,
19 the Δ*mce3R* mutant was attenuated for colonization in a murine model that recapitulates lesions
20 with lipid-rich foamy macrophages. These findings reveal critical coordination between bacterial
21 response to environmental and nutritional cues, and establish Mce3R as a crucial integrator of this
22 process.

23

24 **KEYWORDS**

25 *Mycobacterium tuberculosis*, environmental cues, cholesterol, acidic pH, potassium, lipids,
26 mce3R, foamy macrophages, C3HeB/FeJ.

27

28 **INTRODUCTION**

29 Bacterial colonization of its host requires adaptation of the bacteria to their local
30 environment, which includes ionic signals such as protons (H^+, pH levels), chloride (Cl^-), and
31 potassium (K^+)[1-3]. *Mycobacterium tuberculosis* (Mtb) is the causative agent of tuberculosis, a
32 disease that continues to be a leading cause of death from infectious diseases worldwide[4]. The

33 importance of appropriate sensing and response to the local environment for Mtb is underlined by
34 the substantial attenuation in colonization ability of a mutant deleted for *phoPR*[5,6], a two-
35 component system essential in the response of Mtb to acidic pH that also plays a significant role
36 in its response to Cl^{-}[1,2]. Indeed, the attenuation of a Δ*phoPR* mutant for host colonization is so
37 marked that it has been pursued as a possible vaccine candidate[7,8]. Environmental cues further
38 change in time and space during infection, and we have previously shown that spatial variations
39 in local pH and Cl^{-} levels exist even within a single lesion, and correlate to Mtb replication status[9].
40 Critically, bacteria are exposed during infection not just to a single signal at a time, but
41 concurrently to multiple cues in their local environment. In the case of Mtb, we have shown that
42 the bacteria have a synergistic transcriptional response to the simultaneous presence of acidic pH
43 and high Cl^{-} concentration ([Cl^{-}]), two signals experienced concurrently within a maturing
44 macrophage phagosome[2]. There is further a relationship between the K^{+} homeostasis of Mtb and
45 its response to acidic pH/high [Cl^{-}], with deletion of the CeoBC K^{+} uptake system impairing the
46 response of Mtb to these two environmental cues and negatively affecting the ability of Mtb to
47 colonize its host[3]. Besides PhoPR regulating Mtb response to both acidic pH and high [Cl^{-}][2], other
48 examples of coordinated regulation in signal response are exemplified by additional key two-
49 component systems such as DosRS(T) (nitric oxide stress and hypoxia) and PrrAB (acidic pH,
50 high [Cl^{-}], nitric oxide stress, hypoxia)[10,11]. Of note, PrrA is essential in Mtb[11,12], while mutants in
51 DosRS(T) show significant attenuation in several animal models of Mtb infection[13-15]. These data
52 emphasize the existence of interconnections between environmental signals, and the importance
53 of coordination in response to these signals for successful host colonization by Mtb.
54 Alongside environmental stimuli, the availability of nutrients also plays a crucial role in
55 bacterial adaptation to its host. Particularly for Mtb, cholesterol has been shown to be a major

56 carbon source during infection, with Mtb mutants deficient in their ability to utilize cholesterol
57 attenuated for host colonization[16,17]. Strikingly, Mtb exhibits improved growth in acidic pH media
58 when cholesterol or fatty acids are provided as carbon sources[18,19]. Further, the transcriptional
59 response of Mtb to Cl^- was increased in the simultaneous presence of cholesterol[20]. In addition,
60 two studies have found that iron limitation increases expression of the cholesterol utilization genes
61 in Mtb[21,22]. Together, these data suggest the presence of intrinsic links between Mtb response to
62 environmental (ionic) cues and its metabolism. However, the nature of these relationships and the
63 regulatory factors that underlie them remain largely unexplored and unknown.

64 Here, building on our previous finding that disruption of Mtb K^+ homeostasis decreases
65 the bacterial response to acidic pH and high [Cl^-][3], we first discover that limiting environmental
66 K^+ levels also dampen Mtb response to acidic pH. Exploitation of a pH reporter Mtb-based
67 transcription factor overexpression screen then unexpectedly revealed a connection between Mtb
68 lipid metabolism regulation with control of the bacterial pH response in the presence of limiting
69 [K^+]. Focusing on the putative lipid utilization regulator Mce3R, overexpression of *mce3R*
70 partially rescued, while *mce3R* deletion conversely further repressed, the acidic pH response of
71 Mtb in the presence of low external [K^+]. The presence of cholesterol was found to increase Mtb
72 transcriptional response to low [K^+], with global transcriptional analyses demonstrating that Mtb
73 response to acidic pH was also augmented in the simultaneous presence of cholesterol and vice
74 versa. Strikingly, deletion of *mce3R* resulted in loss of augmentation of the cholesterol response
75 in the presence of acidic pH, while having minimal effect on Mtb transcriptional response to
76 cholesterol or acidic pH alone. Similarly, augmentation of the low [K^+] response by the
77 simultaneous presence of cholesterol was lost in the Δ*mce3R* Mtb mutant. Lastly, we show that
78 deletion of *mce3R* had significant consequences for Mtb host colonization, with the Δ*mce3R*

79 mutant attenuated for growth in foamy macrophages and colonization of C3HeB/FeJ mice during
80 a six-week infection. Together, our findings reveal the intrinsic interconnections between Mtb
81 response to acidic pH, low [K^+], and cholesterol, and establish Mce3R as a critical mechanism
82 through which integration of these signals is accomplished in Mtb.
83
84 **RESULTS**
85 **Environmental K^+ levels modulate Mtb transcriptional response to acidic pH**
86 To investigate the impact of environmental potassium (K^+) levels on the response of Mtb
87 to acidic pH, we exposed our previously established pH-responsive Mtb reporter, *rv2390c'*::GFP[2],
88 to standard 7H9, pH 7 medium, or 7H9, pH 5.85 medium with sufficient K^+ (7.6 mM) or a K^+
89 concentration limited to 0.1 mM. As shown in Figure 1A, K^+ limitation strikingly decreased the
90 induction of *rv2390c'*::GFP fluorescence signal observed at acidic pH. This decrease in acidic pH
91 response was further [K^+]-dependent, with increased dampening of reporter induction with
92 decreasing [K^+] (Figure 1B). Importantly, this effect of K^+ limitation on the acidic pH response of
93 Mtb was unidirectional, as the bacterial response to low [K^+], tested using the K^+ reporter Mtb
94 strain *kdpF'*::GFP[3], was not influenced by changes in environmental pH (Figure 1C).
95 Together, these assays reveal a previously unknown impact of environmental [K^+] levels
96 on the response of Mtb to acidic pH.
97
98 **Lipid utilization regulators modulate the interplay between environmental [K^+] and Mtb pH**
99 **response**
100 To investigate the regulatory mechanism(s) underlying the relationship between
101 environmental [K^+] and the acidic pH response of Mtb, a screening approach was employed using

102 an arrayed inducible transcription factor overexpression library generated in the background of a
103 pH-responsive *rv2390c'*::luciferase reporter[11]. 7H9, pH 7, 0.05 mM K^+ or 7H9, pH 5.85, 1.6 mM
104 K^+ media served as negative and positive control conditions respectively, with an empty vector
105 control included. Two K^+ limiting concentrations, 0.1 and 0.05 mM, both at pH 5.85, were used
106 as the test conditions. The fold induction of *rv2390c'*::luciferase reporter signal in each test
107 condition compared to the negative control was calculated as relative light units (RLU)/OD_{600} to
108 account for any variations in bacterial growth. The arrayed set-up of the screen removed any
109 concerns of bottleneck effects and enabled immediate identification of hits of interest.

110 Unexpectedly, a key class of hits identified from the screen were regulators involved in
111 lipid (cholesterol or fatty acid) metabolism (Figure 2A, Table S1). In particular, overexpression of
112 *rv1219c* and *mce3R* partially rescued the dampening of *rv2390c'*::luciferase signal at pH 5.85 with
113 limiting [K^+] (Figure 2A, Table S1). Conversely, overexpression of *mce1R*, *kstR*, *mce2R*, *rv1129c*,
114 and *rv1816* repressed *rv2390c'*::luciferase induction even more compared to the empty vector
115 control (Figure 2A, Table S1). These phenotypes were first validated by comparing uninduced
116 (ethanol, EtOH) conditions versus induced (200 ng/ml anhydrotetracycline, ATC) conditions for
117 each transcription factor overexpression strain, with outcomes consistent with the screen results
118 (comparison to empty vector) obtained in all cases (Figure 2B). As noted above, these seven
119 transcription factors are known or predicted to be involved in lipid metabolism. Specifically,
120 *mce1R, mce2R*, *rv1219c*, and *rv1816* have previously been shown to be involved in fatty acid
121 metabolism[23-27], *kstR* is a key regulator of cholesterol β-oxidation[28,29], and *rv1129c* is involved in
122 propionyl-CoA metabolism[30]. *mce3R* is predicted to be involved in lipid metabolism due to its
123 homology to the other Mce complexes[31-34].

124 We decided to pursue here further study of Mce3R, given its still poorly understood role
125 in Mtb biology. A deletion mutant strain of *mce3R* was generated and tested in the same
126 experimental conditions as in the original *rv2390c'*::luciferase transcription factor overexpression
127 screen. As shown in Figure 2C, in contrast to overexpression of *mce3R* which partially rescued the
128 Mtb pH response phenotype in the presence of low [K^+], deletion of *mce3R* resulted in the converse
129 phenotype, with a significant reduction in pH regulon gene expression in the mutant strain in acidic
130 pH + K^+-limiting conditions, compared to the parental wild type (WT) strain. Complementation
131 of the Δ*mce3R* strain restored gene induction to WT levels (Figure 2C).

132 Taken together, these results indicate that factors related to lipid metabolism regulation
133 play a role in modulating the interplay between external K^+ levels and the response of Mtb to the
134 critical environmental cue of acidic pH.

135

136 **Mtb transcriptional response to acidic pH, low [K^+], and cholesterol are linked**

137 Given the intriguing connection revealed by the screen between Mtb lipid metabolism
138 regulation, acidic pH response, and environmental [K^+], we next pursued investigation of how
139 these three facets might be related at the transcriptional level. Examination of the impact of K^+
140 limitation on the transcriptional response of Mtb to cholesterol showed that it also dampened
141 induction of the five tested Mtb cholesterol regulon genes (Figure 3A). Interestingly, we also
142 observed a reverse association, where cholesterol further induced the expression of genes in the
143 K^+ regulon, in the presence of K^+-limiting conditions (Figure 3B). These data relate the presence
144 of cholesterol to environmental K^+, further supporting a complex interplay between lipid
145 metabolism, environmental K^+ levels, and Mtb response to acidic pH.

146 To obtain a comprehensive understanding of the interplay between the transcriptional
147 response of Mtb to acidic pH and cholesterol, we conducted genome-wide RNA sequencing
148 (RNAseq) analysis, with Mtb exposed to conditions of: (i) 7H9, pH 7 (control), (ii) 7H9, pH 5.7,
149 (iii) cholesterol, pH 7, and (iv) cholesterol, pH 5.7 media. Examination of the impact of acidic pH
150 on the response of Mtb to cholesterol showed an augmentation in the induction of a subset of
151 genes, with expression of 25 differentially expressed genes increased (genes differentially
152 expressed $\log_2$-fold change ≥ 1 in the cholesterol, pH 7 condition; $\log_2$-fold change ≥ 0.6 between
153 cholesterol, pH 5.7 and cholesterol, pH 7 conditions; $p<0.05$, FDR<0.01 in both sets) (Figure 4A,
154 Table S2). Further analysis by qRT-PCR indicated a stepwise concentration dependence in this
155 relationship, with expression levels of the cholesterol regulon genes tested showing distinct
156 increase levels with increasing acidity (Figure 4B). On the other hand, increasing the concentration
157 of cholesterol smoothly increased induction levels of the tested genes in both pH 7 and pH 5.7
158 conditions (Figure 4C).

159 Complementarily, the RNAseq data showed that the presence of cholesterol also affected
160 differential gene expression of Mtb in response to acidic pH (Figure 4D, Table S3). In this case,
161 the presence of cholesterol increased expression of a subset of pH regulon genes, with expression
162 of 118 differentially expressed gene increased (genes differentially expressed $\log_2$-fold change ≥ 1
163 in the pH 5.7 condition; $\log_2$-fold change ≥ 0.6 between cholesterol, pH 5.7 and 7H9, pH 5.7
164 conditions; $p<0.05$, FDR<0.01 in both sets), but also interestingly reduced expression of a different
165 subset of genes, with 67 differentially expressed gene decreased (gene differentially expressed
166 $\log_2$-fold change ≥ 1 in the pH 5.7 condition; $\log_2$-fold change ≥ 0.6 between cholesterol, pH 5.7
167 and 7H9, pH 5.7 conditions; $p<0.05$, FDR<0.01 in both sets) (Figure 4D, Table S3). Among this
168 latter group, further examination of the RNAseq data showed that the majority of genes (35/43)

169 most strongly affected (log_2-fold change ≥1.59 between cholesterol, pH 5.7 and 7H9, pH 5.7
170 conditions) also exhibited lower expression in the cholesterol, pH 7 condition compared to 7H9,
171 pH 7. As such, the presence of cholesterol alone downregulates expression of these genes. This
172 finding indicates an overlap in a subset of the cholesterol and pH regulon in Mtb; expression of
173 these genes is regulated in opposite directions by the two signals when present individually
174 (induced by acidic pH, repressed by cholesterol), with cholesterol appearing to be the dominant
175 signal when Mtb is exposed to both cues concurrently.

176 Focusing on genes in the acidic pH regulon that are not also differentially expressed in the
177 presence of cholesterol alone, qRT-PCR analysis showed a concentration dependence in the
178 augmentation of gene expression induction at acidic pH with increasing cholesterol concentration
179 (Figure 4E). pH level-dependence of induction of the acidic pH regulon genes tested was also
180 observed in both standard 7H9 and cholesterol conditions (Figure 4F). Overall, these findings
181 show the global cross-regulation between cholesterol and pH response in Mtb, with the concurrent
182 presence of each factor strongly influencing the expression of genes in each regulon.

183

184 **Mce3R regulates Mtb response to cholesterol only in the context of acidic pH**

185 Our results above raise the question of how Mtb response to acidic pH and cholesterol is
186 cross-regulated. To gain insight into possible regulatory mechanisms underlying the synergy in
187 Mtb transcriptional response to cholesterol and acidic pH in the concurrent presence of both cues,
188 we first tested the effect of a *phoPR* deletion on these responses. PhoPR is a well-established two-
189 component system known to play a crucial role in Mtb response to the linked environmental cues
190 of acidic pH and Cl^-[1,2]. Consistent with this, we observed that a Δ*phoPR* mutant exhibited
191 significantly reduced induction of acidic pH regulon genes in both standard 7H9 or cholesterol

192 media as a base (Figure S1A). Notably however, the simultaneous presence of cholesterol still
193 resulted in an increase in the induction level of several tested genes, compared to the single acidic
194 pH condition, in Δ*phoPR* Mtb (Figure S1A, compare open red bars to open black bars). The same
195 phenomenon of an overall decrease in gene expression induction with the Δ*phoPR* Mtb mutant in
196 both standard 7H9 or cholesterol media as a base was also observed with Cl^- as the inducing signal
197 instead of acidic pH (Figure S1B). Similarly, the continued increase in gene expression induction
198 for a few tested genes in the simultaneous presence of cholesterol was also observed in the dual
199 cholesterol/high [Cl^-] condition compared to the single high [Cl^-] condition (Figure S1B, compare
200 open blue bars to open black bars). Complementation of the Δ*phoPR* Mtb mutant restored gene
201 expression profiles to WT levels in all cases (Figure S1). These findings suggest the involvement
202 of additional regulators that contribute to the coordination of the acidic pH/Cl^- response with Mtb
203 response to cholesterol.

204 The putative lipid metabolism regulator Mce3R had been found as a robust hit in the
205 transcription factor overexpression library screen described above, which first revealed the ability
206 of lipid metabolism regulators to modulate the interplay between environmental K^+ levels and the
207 response of Mtb to acidic pH. While Mce3R is known to regulate the *mce3* operon and associated
208 upstream genes[31-33], its possible role in the overall response of Mtb to cholesterol is unknown. To
209 determine if Mce3R might also play a role in coordinating Mtb acidic pH and cholesterol response,
210 we performed global RNAseq analysis on the Δ*mce3R* mutant and compared the transcriptional
211 profiles obtained to those of WT Mtb. The same four conditions utilized above for WT Mtb were
212 used here, namely: (i) 7H9, pH 7 (control), (ii) 7H9, pH 5.7, (iii) cholesterol, pH 7, and (iv)
213 cholesterol, pH 5.7 media. A first observation was that *mce3R* deletion had little effect on global
214 transcriptional response of Mtb to acidic pH or cholesterol when either condition was present alone

215 (Figures 5A and 5B, Tables S4 and S5). Strikingly however, in the dual cholesterol, pH 5.7
216 condition, a subset of genes associated with the cholesterol regulon were significantly less induced
217 in the Δ*mce3R* Mtb mutant compared to WT (Figure 5C, Table S6). Follow-up qRT-PCR
218 experiments validated that *mce3R* deletion only affected expression of cholesterol regulon genes
219 in Mtb in the context of the simultaneous presence of cholesterol and acidic pH, with
220 complementation restoring gene expression to WT levels (Figures 5D and 5E). Markedly, for the
221 Δ*mce3R* mutant, the induction levels of the cholesterol regulon genes in the dual cholesterol, pH
222 5.7 condition were very similarly to those observed in the single cholesterol (pH 7) condition
223 (compare open bars in Figure 5E to open bars in Figure 5D). Of note, augmentation in expression
224 of acidic pH regulon genes by cholesterol was however still observed in the Δ*mce3R* mutant as
225 compared to WT Mtb (Figure 5F).

226 Given (i) the results above, (ii) our finding that cholesterol also augments Mtb response to
227 low [K^+] (Figure 3B), and (iii) the original identification from our screen of Mce3R as a regulator
228 able to modulate the interplay between environmental K^+ levels and the response of Mtb to acidic
229 pH, we next sought to test if Mce3R would also have a role in coordinating Mtb response in the
230 simultaneous presence of both cholesterol and low [K^+]. WT, Δ*mce3R*, and the complemented
231 Δ*mce3R* Mtb mutant (*mce3R**) were exposed to: (i) K^+-free 7H9, pH 7, or (ii) K^+-free cholesterol,
232 pH 7 media, for 4 hours before RNA were extracted for gene expression analysis. Strikingly, the
233 ability of cholesterol to augment induction of the K^+ regulon genes was largely lost in the Δ*mce3R*
234 mutant, even as deletion of *mce3R* had no effect on induction of the K^+ regulon genes in the
235 absence of cholesterol (Figure 6A). The dampening of cholesterol gene induction by the
236 simultaneous presence of low [K^+] was additionally unchanged by deletion of *mce3R* (Figure 6B).

237 Together, these results excitingly identify Mce3R as a transcription factor that specifically
238 acts to coordinate Mtb response in the presence of at least two environmental signals (cholesterol
239 + acidic pH, low [K^+] + cholesterol, acidic pH + low [K^+]), with little effect when only one signal
240 is present. There is further directionality in its activity, as in each case, *mce3R* deletion affected
241 response to only one of the two signals concurrently present. These findings emphasize the
242 interconnectedness between Mtb response to acidic pH, low [K^+], and cholesterol, and the
243 multifaceted role of Mce3R in the coordinated regulation of Mtb response to its local environment.
244

245 **A Δ*mce3R* Mtb mutant is attenuated for host colonization in the presence of lipids**

246 Changes in pH and [K^+], and differing presence of cholesterol, are all factors expected to
247 occur during Mtb host colonization. To assess the importance of Mce3R during infection, we
248 infected bone marrow-derived macrophages (BMDMs) with WT, Δ*mce3R*, or *mce3R** Mtb. Given
249 our findings of the importance of Mce3R in coordination of the cholesterol response of Mtb, these
250 infections were also performed in BMDMs pre-treated with oleate to induce the formation of
251 foamy macrophages[35,36], to determine whether infection in lipid-rich macrophages would differ
252 from untreated BMDMs. As shown in Figure 7A, the Δ*mce3R* mutant was attenuated for growth
253 in BMDMs compared to the WT and *mce3R** Mtb, with a more pronounced effect in the context
254 of foamy macrophage infection. While Mtb actively prevents complete maturation of the
255 phagosome, it is still exposed to slightly decreased pH levels during macrophage infection[37]. These
256 results thus support a role of Mce3R in the ability of Mtb to respond appropriately to its local
257 environment for continued growth.

258 Finally, we examined the role of Mce3R in Mtb infection of a whole animal host using the
259 C3HeB/FeJ murine model. Importantly, this mouse strain recapitulates key lesion types observed

260 during human infection[38-40]. Of pertinence here, foamy macrophages are present at 6 weeks post-
261 infection, both in macrophage-rich lesions and in the cuff surrounding caseous necrotic lesions
262 that are the hallmark of tuberculosis disease (Figure 7B)[41]. The mice were infected with WT,
263 Δ*mce3R*, or *mce3R** Mtb, and the infection allowed to progress for 2 or 6 weeks. We did not
264 observe significant differences in bacterial load among the three strains at the 2-week time point
265 (Figure 7C), consistent with this time point being prior to the formation of foamy macrophages
266 (Figure 7B). In contrast, at the 6-week time point, the Δ*mce3R* mutant exhibited a significantly
267 reduced bacterial load compared to the WT and *mce3R** Mtb strains (Figure 7C).

268 Together, these results demonstrate that Mce3R plays an important role in Mtb growth in
269 macrophages, with the absence of Mce3R resulting in a significantly reduced ability of Mtb to
270 maintain persistent colonization of a whole animal host.

271

272 **DISCUSSION**

273 From the alveolar airspace to the macrophage phagosome to the granuloma, Mtb
274 encounters a complex and dynamic environmental milieu that plays a crucial role in shaping its
275 infection biology. This milieu encompasses signals originating from the cellular and tissue
276 microenvironment, which often reflect the host's immune response, and changes to available
277 nutrient sources. There have been extensive studies seeking to understand the response of Mtb to
278 specific environmental signals and nutrients, and the regulation underlying such responses. In
279 contrast, significantly less is known regarding the interplay between Mtb response to particular
280 environmental stimuli and available nutrients, and the regulatory mechanisms that enable the
281 integration of such responses. Our study here reveals the intrinsic relationships between Mtb
282 response to low [K^+], acidic pH, and cholesterol, with synergy in the acidic pH and cholesterol

283 response, and dampening of Mtb response to both signals in the presence of low [K^+]. Concurrent
284 exposure to acidic pH and cholesterol is expected to be a critical aspect of the local environment
285 during Mtb infection, in the context of bacterial residence in phagosomes of foamy macrophages,
286 a major host cell type observed not just in animal models of infection, but also in human
287 infections[38,39,42,43]. Indeed, Mtb growth in acidic pH media is improved when cholesterol is
288 provided as the carbon source[18], and our finding of synergy in Mtb transcriptional response to
289 these two signals provides a crucial new dimension to the understanding of Mtb adaptive biology
290 in this environment.

291 Changes in expression of bacterial "virulence factors", driven by changes in the presence
292 of specific metabolites, have been increasingly described for different bacterial pathogens[44]. This
293 includes increased expression of leucocidins in *Staphylococcus aureus* in the presence of
294 pyruvate[45], and induced expression of *Salmonella* pathogenicity island 2 genes in the presence of
295 succinate[46]. Our results demonstrating the reciprocal augmentation of Mtb response to acidic pH
296 and cholesterol in the concurrent presence of both signals, and the increased expression of K^+-
297 responsive genes in the simultaneous presence of cholesterol, expands on this facet of bacterial
298 biology. In particular, together with previous studies that have shown increased transcription of
299 genes in the Cl^- regulon in the simultaneous presence of cholesterol[20], and increased expression of
300 cholesterol utilization genes in iron-limiting conditions[21,22], our findings support the existence of
301 an intrinsic interplay between Mtb response to environmental cues and the critical nutrient of
302 cholesterol.

303 Strikingly, we identify Mce3R as a transcription factor that critically functions in the
304 integration of these signals. Specifically, a Δ*mce3R* mutant fails to synergistically upregulate genes
305 in the cholesterol regulon in the simultaneous presence of acidic pH, and in the K^+ regulon in the

306 simultaneous presence of cholesterol, even while response to each signal individually is
307 unaffected. It will be intriguing in future studies to explore the underlying mechanism enabling
308 the triggering of Mce3R function only in the context of the concurrent presence of two signals
309 versus one. Mce3R is a cytoplasmic protein and would not directly sense changes in external
310 signals, although an increase in cholesterol utilization would result in increased levels of
311 cholesterol within the bacterium. Of note, the affinity of Mce2R and Mce1R for binding to their
312 target DNA have been reported (experimentally or computationally respectively) to change in the
313 presence of long-chain fatty acids[25,47]. Whether and how Mce3R binding to DNA may be affected
314 by cholesterol, and whether interacting partners exist that aid in transducing the external stimuli to
315 Mce3R, are thus areas for future investigation. In addition, a recent report indicated that a Δ*mce3R*
316 Mtb mutant was less susceptible to oxidative stress[48], a host defense response also encountered by
317 the bacteria during infection of phagocytes[49]. Further studies are required to determine if Mce3R
318 may also act in integrating oxidative stress signals with cholesterol response in Mtb.

319 As in mammalian cells, K^+ is also the most abundant cation in bacterial cells, and the
320 importance of K^+ in host colonization is becoming increasingly appreciated[3,50,51]. Our unexpected
321 finding linking Mtb lipid utilization regulators to the bacterium's K^+ response opens a new facet
322 of study in understanding how K^+ response/homeostasis integrates with the metabolism of a
323 bacterium. Intriguingly, cholesterol regulation of K^+ channel activity has been demonstrated in
324 mammalian systems, with the inwardly rectifying K^+ (Kir) channels shown to possess cholesterol-
325 binding sites[52,53]. Regulation of the prokaryotic homolog of Kir (KirBac1.1) by cholesterol has
326 also been demonstrated[54]. Cholesterol binding usually downregulates Kir channel function,
327 although it has been shown to enhance activity of certain Kir channels, such as Kir3.4[55]. In Mtb,
328 the CeoBC K^+ uptake system is critical in maintaining K^+ homeostasis[3,56]. Whether cholesterol

329 directly regulates CeoBC activity in Mtb, and more broadly K^+ uptake systems in other pathogens,
330 is an interesting question for future study.

331 Exposure to different environmental signals with a simultaneous change in available
332 nutritional source is a widespread phenomenon for bacterial pathogens and not unique to Mtb. We
333 propose that further study of bacterial responses to concurrent environmental and nutritional cues
334 will yield important new insight into bacterial signal integration and their underlying mechanisms.
335 Unique nodes represented by regulatory factors that specifically act to coordinate bacterial
336 environmental response to multiple signals and thus adaptation, such as Mce3R as identified here,
337 further represent exciting new candidates for therapeutic targeting[57].

338

339 **ACKNOWLEDGEMENTS**

340 We thank members of the Tan laboratory for helpful discussion, and Trever Smith for initial
341 assistance with RNA sequencing analysis. This work was supported by grants from the National
342 Institutes of Health (R01 AI143867 and R21 AI171356) to ST, and by a Natalie V. Zucker
343 Research Center for Women Scholars Research Award from Tufts University School of Medicine
344 to YC.

345

346 **AUTHOR CONTRIBUTIONS**

347 Conceptualization, YC. and ST.; Investigation, YC, NJM, and ST; Writing – original draft, YC
348 and ST; Writing – review and editing, YC, NJM., and ST; Supervision, ST.; Funding acquisition,
349 YC and ST.

350

351 **DECLARATION OF INTERESTS**

352 The authors declare no competing interests.

353

354 **FIGURE LEGENDS**

355 **Figure 1. Environmental K^+ levels modulate Mtb transcriptional response to acidic pH.** (A)
356 *rv2390c'*::GFP reporter response to acidic pH is dampened in the presence of low [K^+].
357 Mtb(*rv2390c*'::GFP) was grown in 7H9, pH 7.0 or pH 5.85 media, or in K^+-free 7H9, pH 5.85
358 medium, supplemented with 0.1 mM K^+. Samples were taken at indicated time points, fixed, and
359 GFP induction analyzed by flow cytometry. Data are shown as means ± SD from 3 experiments.
360 p-values were obtained with an unpaired t-test with Welch's correction, and compare the 7H9, pH
361 5.85 to the 0.1 mM K^+, pH 5.85 condition. ** $p<0.01$. (B) Dampening of Mtb response to acidic
362 pH by low K^+ is concentration dependent. Mtb(*rv2390c*'::GFP) was grown in 7H9, pH 5.85
363 medium ("control"), or in K^+-free 7H9, pH 5.85 medium, supplemented with indicated amounts
364 of K^+. Samples were taken 9 days post-assay start, fixed, and GFP induction analyzed by flow
365 cytometry. Data are shown as means ± SD from 3 experiments. (C) Mtb response to low [K^+] is
366 not affected by environmental pH. Mtb(*kdpF*'::GFP) was grown in 7H9, pH 7.0 or pH 5.7, or in
367 K^+-free 7H9, pH 7 or pH 5.7 media. Samples were taken at indicated time points, fixed, and GFP
368 induction analyzed by flow cytometry. Data are shown as means ± SD from 3 experiments.

369

370 **Figure 2. A *rv2390c*'::luciferase reporter transcription factor overexpression screen**
371 **identifies lipid utilization regulators as modulators of the interplay between environmental**
372 **[K^+] and Mtb pH response.** (A and B) Lipid utilization regulator hits from reporter-based,
373 inducible transcription factor (TF) overexpression screen. A library of inducible TF
374 overexpression plasmids (P_1'::*TF*-FLAG-tetON) in the background of a Mtb(*rv2390c*'::luciferase)

375 strain was screened for their response to acidic pH in the presence of low [K^+]. TF overexpression
376 was induced by adding 200 ng/ml of anhydrotetracycline (ATC) 1 day before Mtb was exposed to
377 K^+-free 7H9, pH 7 or K^+-free 7H9, pH 5.85 media supplemented with 1.6 mM or 0.05 mM K^+. 9
378 days post-exposure (continuous ATC presence), light output (relative light units, RLU) and OD_{600}
379 were measured. Fold induction compares RLU/OD_{600} in each condition to RLU/OD_{600} in the
380 control K^+-free 7H9, pH 7 condition. (A) shows results of the lipid utilization regulator hits,
381 together with an empty vector plasmid control. (B) shows validation of the screen hits in (A), with
382 each hit TF compared to its uninduced control (ethanol, "EtOH", as a carrier control). In (B), data
383 are shown as means ± SD from three experiments, and p-values were obtained with an unpaired t-
384 test with Welch's correction. N.S. not significant, * $p<0.05$, ** $p<0.01$, *** $p<0.001$, ****
385 $p<0.0001$. (C) Mce3R modulates the interplay between environmental [K^+] and Mtb pH response.
386 Log-phase WT, Δ*mce3R* and *mce3R** (complemented mutant) were exposed for 4 hours to K^+-free
387 7H9, pH 7 or K^+-free 7H9, pH 5.85 media supplemented with 1.6 mM or 0.05 mM K^+, before
388 RNA was extracted for qRT-PCR analysis. Fold change is as compared to the K^+-free 7H9, pH 7
389 condition. *sigA* was used as the control gene, and data are shown as means ± SD from 3 technical
390 replicates, representative of 3 experiments. p-values were obtained with an unpaired t-test with
391 Welch's correction and Holm-Sidak multiple comparisons, N.S. not significant, *** $p<0.001$,
392 **** $p<0.0001$.
393
394 **Figure 3. Mtb transcriptional response to low [K^+] and cholesterol are linked.** (A) Low [K^+]
395 dampens Mtb response to cholesterol. Log-phase Mtb was exposed for 4 hours to (i) 7H9, pH 7,
396 (ii) cholesterol, pH 7, or (iii) K^+-free cholesterol, pH 7 media, before RNA was extracted for qRT-
397 PCR analysis. (B) Cholesterol augments Mtb response to low [K^+]. Log-phase Mtb was exposed

398 for 4 hours to (i) 7H9, pH 7, (ii) K^+-free 7H9, pH 7, or (iii) K^+-free cholesterol, pH 7 media, before
399 RNA was extracted for qRT-PCR analysis. Fold change is as compared to the 7H9, pH 7 condition
400 in all cases. *sigA* was used as the control gene, and data are shown as means ± SD from 3 technical
401 replicates, representative of 3 experiments. p-values were obtained with an unpaired t-test with
402 Welch's correction, *** $p<0.001$, **** $p<0.0001$.
403
404 **Figure 4. Mtb transcriptional response to acidic pH and cholesterol are linked globally.** (A
405 and D) Global changes in Mtb response to cholesterol and acidic pH in the simultaneous presence
406 of both signals. Log-phase Mtb was exposed for 4 hours to (i) 7H9, pH 7, (ii) 7H9, pH 5.7, (iii)
407 cholesterol, pH 7, or (iv) cholesterol, pH 5.7 media, before RNA was extracted for RNAseq
408 analysis. Log_2-fold change compares gene expression in each indicated condition to the 7H9, pH
409 7 condition. Genes marked in red had a log_2-fold change ≥ 0.6 between the two conditions
410 compared ($p<0.05$, FDR<0.01 in both sets, with log_2-fold change ≥1 in the single condition set).
411 (B and C) Effect of acidic pH on Mtb response to cholesterol is concentration dependent. Log-
412 phase Mtb was exposed to the indicated conditions, along with control 7H9, pH7 condition, for 4
413 hours, before RNA was extracted for qRT-PCR analysis. (E and F) Effect of cholesterol on Mtb
414 response to acidic pH is concentration dependent. For all qRT-PCR data, fold change is as
415 compared to the 7H9, pH 7 condition, and data are shown as means ± SD from 3 technical
416 replicates, representative of 3 experiments.
417
418 **Figure 5. Mce3R regulates Mtb response to cholesterol only in the context of acidic pH.** Log-
419 phase WT, Δ*mce3R* and *mce3R** (complemented strain) Mtb were exposed for 4 hours to (i) 7H9,
420 pH 7, (ii) 7H9, pH 5.7, (iii) cholesterol, pH 7, or (iv) cholesterol, pH 5.7 media, before RNA was

421 extracted for RNAseq (A-C) or qRT-PCR (D-F). For RNAseq data, $\log_2$-fold change compares
422 gene expression in each indicated condition to the 7H9, pH 7 condition. Genes marked in red had
423 a $\log_2$-fold change ≥ 0.6 between Δ*mce3R* and WT strains in the indicated condition ($p<0.05$,
424 FDR<0.01 in both sets, with $\log_2$-fold change ≥1 in WT). For qRT-PCR data, fold change is as
425 compared to the 7H9, pH 7 condition. Data are shown as means ± SD from 3 technical replicates,
426 representative of 3 independent experiments. p-values were obtained with as unpaired t-test with
427 Welch's correction and Holm-Sidak multiple comparisons. N.S. not significant, ** $p<0.01$, ***
428 $p<0.001$, **** $p<0.0001$.
429
430 **Figure 6. Mce3R deletion dampens Mtb response to K^+ in the presence of cholesterol**. Log-
431 phase WT, Δ*mce3R*, and *mce3R** (complemented strain) Mtb were exposed for 4 hours to (A) K^+-
432 free 7H9 or cholesterol media at pH 7, or (B) cholesterol or K^+-free cholesterol media at pH 7,
433 along with 7H9, pH 7 as the control condition. Fold change is as compared to the 7H9, pH 7
434 condition in all cases. *sigA* was used as the control gene, and data are shown as means ± SD from
435 3 technical replicates, representative of 3 experiments. p-values were obtained with an unpaired t-
436 test with Welch's correction and Holm-Sidak multiple comparisons, N.S. not significant, **
437 $p<0.01$, *** $p<0.001$, **** $p<0.0001$.
438
439 **Figure 7. A Δ*mce3R* Mtb mutant is attenuated for host colonization in the presence of lipids.**
440 (A) Δ*mce3R* Mtb is attenuated for macrophage colonization. Murine bone marrow-derived
441 macrophages untreated or pre-treated with oleate for 24 hours to induce foamy macrophages were
442 infected with WT, Δ*mce3R*, or *mce3R** (complemented mutant) Mtb, and colony forming units
443 (CFUs) tracked over time. Data are shown as means ± SD from 3 wells, representative of 3

444 independent experiments. p-values were obtained with an unpaired t-test with Welch's correction,
445 comparing Δ*mce3R* to WT Mtb in untreated macrophages (*) or foamy macrophages (#). */#
446 p<0.05, ** p<0.01. (B) Mtb is present in foamy macrophages 6 weeks post-infection in C3HeB/FeJ
447 mice. C3HeB/FeJ mice were infected with Mtb constitutively expressing mCherry, and animals
448 sacrificed at 2 or 6 weeks post-infection. Lungs were fixed and processed for confocal microscopy
449 imaging. Images shown are z-slices from reconstructed 3D images. Nuclei are shown in grayscale
450 (DAPI), all bacteria are marked in red (mCherry), f-actin is shown in blue (phalloidin), and lipid
451 droplets are shown in green (Bodipy 493/503). Scale bar 10 µm. (C) Δ*mce3R* Mtb is attenuated
452 for colonization in a murine infection model. C3HeB/FeJ mice were infected with WT, Δ*mce3R*,
453 or *mce3R** Mtb, and lung homogenates plated for CFUs 2 or 6 weeks post-infection. p-values were
454 obtained with a Mann-Whitney statistical test. N.S. not significant, **p<0.01.
455

456 **STAR★Methods**

457 **Key resources table**

REAGENT or RESOURCE	SOURCE	IDENTIFIER
Bacterial strains		
Mycobacterium tuberculosis CDC1551 *rv2390c'*::GFP	[2]	N/A
Mycobacterium tuberculosis CDC1551 *kdpF'*::GFP	[3]	N/A
Mycobacterium tuberculosis CDC1551 *rv2390c'*::luciferase	[11]	N/A
Transcription factor overexpression library in *Mycobacterium tuberculosis* CDC1551 *rv2390c'*::luciferase background	[11]	N/A
Mycobacterium tuberculosis CDC1551 streptomycin-resistant	[2]	N/A
Mycobacterium tuberculosis CDC1551 streptomycin-resistant Δ*phoPR*	[2]	N/A
Mycobacterium tuberculosis CDC1551 streptomycin-resistant *phoPR** (complemented Δ*phoPR* strain)	[2]	N/A

Mycobacterium tuberculosis CDC1551 streptomycin-resistant Δ*mce3R*	This study	N/A
Mycobacterium tuberculosis CDC1551 streptomycin-resistant *mce3R** (complemented Δ*mce3R* strain)	This study	N/A
Mycobacterium tuberculosis Erdman streptomycin-resistant	[3]	N/A
Mycobacterium tuberculosis Erdman streptomycin-resistant Δ*mce3R*	This study	N/A
Mycobacterium tuberculosis Erdman streptomycin-resistant *mce3R** (complemented Δ*mce3R* strain)	This study	N/A
Critical commercial assays		
Bright-Glo luciferase assay system	Promega	E2610
Deposited data		
RNA sequencing data	This study	NCBI GEO: GSE241072
Experimental models: Cell lines		
L-929	ATCC	CCL-1
Experimental models: Organisms/strains		
Mouse: C57BL/6J	Jackson Laboratories	000664
Mouse: C3HeB/FeJ	Jackson Laboratories	000658
Oligonucleotides		
Primer: mce3R-KO-AflII-F1: 5' GCTAGG cttaag GCC TTG TCG GCC ACG ATT ACC AT	This study	N/A
Primer: mce3R-KO-XbaI-R1: 5' GCTAGG tctaga AAT CTG CTT CTT CCG GTC CTT TGG G	This study	N/A
Primer: mce3R-KO-HindIII-F2: 5' GCTAGG aagctt GGC AGG TAA CCT CTT GCG CGC ATA	This study	N/A
Primer: mce3R-KO-SpeI-R2: 5' GCTAGG actagt CCG ACG AAA CGA CGC CGA CAC	This study	N/A
Primer: mce3R-seq-F1: 5' CGT CAT CAA CAC CCC AGG CAG	This study	N/A
Primer: mce3R-seq-R2: 5' GCA GGA GGT GTT GCC GTT CAG	This study	N/A
Primer: mce3R-comp-XbaI-F1: 5' GCTAGG tctaga GTG ATC GGA TGC CGC ATC CTG A	This study	N/A
Primer: mce3R-comp-ClaI-R1: 5' GCTACC atcgat a CTA TGC GCG CAA GAG GTT ACC TGC	This study	N/A
Software and algorithms		

FlowJo	BD	https://www.flowjo.com
Geneious	Geneious	https://www.geneious.com
Prism	GraphPad Software	https://www.graphpad.com
Volocity	Quorum Technologies	https://www.volocity4d.com
Other		
DAPI	Invitrogen	D3571
Bodipy 493/503	Invitrogen	D3922
Alexa Fluor 647 phalloidin	Invitrogen	A22287

Resource availability

Further information and requests for resources and reagents should be directed to and will be fulfilled by the lead contact, Shumin Tan (shumin.tan@tufts.edu).

Materials availability

All newly generated Mtb strains are available on request from the lead contact, to investigators with the necessary biosafety level 3 facilities to receive and work with these materials.

Data and code availability

- All RNA sequencing data have been deposited in the NCBI GEO database (GSE241072).
- This paper does not report original code.
- Any additional information required to reanalyze the data reported in this work paper is available from the lead contact upon request

Experimental model and subject details

Murine strains

475 C57BL/6J and C3HeB/FeJ wild type mice were obtained from Jackson Laboratories. All mice
476 used were female and aged 4 weeks on arrival. Mtb infections were carried out when the mice
477 were 6 weeks of age. All animal protocols in this research followed the guidelines from The
478 National Institutes of Health "Guide for Care and Use of Laboratory Animals". All animal
479 protocols (#B2021-139) were reviewed and approved by the Institutional Animal Care and Use
480 Committee at Tufts University, in accordance with guidelines from the Association for Assessment
481 and Accreditation of Laboratory Animal Care, the US Department of Agriculture, and the US
482 Public Health Service.
483
484 **Method details**
485 **Mtb strains and culture**
486 Mtb cultures were propagated and maintained as previously described[58]. K^+-free and cholesterol
487 media were prepared as previously described[3,20]. All antibiotics were added as appropriate at the
488 following concentrations: 100 µg/ml streptomycin, 50 µg/ml hygromycin, 50 µg/ml apramycin,
489 and 25 µg/ml kanamycin. Strains for *in vitro* assays were in the CDC1551 background, while
490 infection assays were carried out with strains in the Erdman background. The *rv2390c'*::GFP,
491 *kdpF'*::GFP, and *smyc'*::mCherry reporters, and the Δ*phoPR* strain and its complement have all
492 been previously described[2,3]. The Δ*mce3R* mutant and its complement were constructed as
493 previously described[2], with the Δ*mce3R* mutation consisting of a deletion beginning at the *mce3R*
494 start codon (as annotated in the Erdman Mtb strain) through 26 bp from the *mce3R* stop codon.
495 The *rv2390c'*::luciferase transcription factor overexpression library has been previously
496 described[11].
497

498 **Reporter Mtb strain broth assays**

499 Reporter strains at log-phase were subcultured to an OD_{600} = 0.05 and resuspended in the
500 appropriate media. These were: (i) 7H9, pH 7, (ii) 7H9, pH 5.85, and (iii) K^+-free 7H9
501 supplemented with 0.1 mM K^+, pH 5.85, for assays with the *rv2390c'*::GFP reporter. For assays
502 with the *kdpF'*::GFP reporter, media conditions were: (i) 7H9, pH 7, (ii) 7H9, pH 5.7, (iii) K^+-free
503 7H9, pH 7, and (iv) K^+-free 7H9, pH 5.7. For broth assays conducted in K^+-free media, an
504 additional wash step with K^+-free 7H9, pH 7 medium was performed prior to resuspending the
505 cultures in the final assay media. At each time point, aliquots of the cultures were taken and fixed
506 in 4% paraformaldehyde (PFA) in phosphate-buffered saline (PBS). Reporter GFP signal was
507 measured using a BD FACSCalibur flow cytometer, and the data analyzed using FlowJo software
508 (BD).

509

510 ***rv2390c'*::luciferase transcription factor overexpression library screen**

511 To screen the *rv2390c'*::luciferase, tetracycline-inducible transcription factor overexpression
512 (TFOE) library, thawed TFOE Mtb strains in 96-well plates (35 µl volume) were mixed with 165
513 µl of 7H9, pH 7 medium supplemented with 25 µg/ml kanamycin and 50 µg/ml hygromycin. The
514 plates were then incubated for 11 days at 37°C in a 5% CO_2 incubator. Subsequently, the TFOE
515 *rv2390c'*::luciferase strains were subcultured at a 1:10 dilution into 100 µl of fresh 7H9, pH 7
516 medium with appropriate antibiotics and incubated for an additional eight days. After eight days
517 of growth, 200 ng/ml anhydrotetracycline (ATC) was added to induce overexpression of each
518 transcription factor for 24 hours. Following the induction, all samples were transferred to a 96-
519 well v-bottom plate (Corning Costar) and pelleted at 3,000 rpm for 10 minutes. The samples were
520 then washed once with K^+-free 7H9, pH 7. Each strain was then inoculated at a 1:10 dilution into

521 100 µl of the following media conditions: (i) K^+-free 7H9, pH 7, supplemented with 0.05 mM KCl,
522 (ii) K^+-free 7H9, pH 5.85, supplemented with 1.6 mM KCl, (iii) K^+-free 7H9, pH 5.85,
523 supplemented with 0.1 mM KCl, and (iv) K^+-free 7H9, pH 5.85, supplemented with 0.05 mM KCl,
524 in clear-bottom white 96-well plates (Corning Costar). The cultures were then incubated for nine
525 days at 37°C in a 5% CO_2 incubator. All media contained 50 µg/ml hygromycin and 25 µg/ml
526 kanamycin, as well as 200 ng/ml ATC for continued transcription factor overexpression.
527 Following this nine day incubation, luminescence was assessed using the Bright-Glo luciferase
528 assay system (Promega) as previously described, with both the light output (relative light units,
529 RLU), and the OD_{600} measured using a Biotek Synergy Neo2 multi-mode microplate reader[11].
530 Fold induction was determined by comparing the RLU/OD_{600} values of the samples from each
531 environmental condition to the RLU/OD_{600} value of Mtb in the K^+-free 7H9, pH 7, 0.05 mM KCl
532 control condition.
533
534 **RNA sequencing and qRT-PCR analyses**
535 For RNA sequencing (RNAseq) and qRT-PCR analyses, log-phase Mtb cultures (OD_{600} ~0.6)
536 were used to inoculate standing T25 flasks with filter caps at an OD_{600} = 0.3, containing 10 ml of
537 the following media: (i) 7H9, pH 7.0, (ii) 7H9, pH 5.7, (iii) cholesterol, pH 7.0, or (iv) cholesterol,
538 pH 5.7. For transcriptional analysis of Mtb under K^+-free conditions, an additional wash step with
539 K^+-free 7H9, pH 7, was performed prior to inoculation of the culture into the various test
540 conditions: (i) K^+-free 7H9, pH 7, supplemented with 0.05 mM KCl (control), (ii) K^+-free 7H9,
541 pH 5.85, supplemented with 1.6 mM KCl, (iii) K^+-free 7H9, pH 5.85, supplemented with 0.1 mM
542 KCl, or (iv) K^+-free 7H9, pH 5.85, supplemented with 0.05 mM KCl. After four hours of exposure
543 to the specific environmental conditions, Mtb samples were collected and RNA isolated as

544 previously described[1]. For RNAseq, two biological replicates were prepared for each condition.
545 Library preparation was performed by the Tufts University Genomics Core Facility using the
546 Illumina stranded total RNA with Ribo-Zero Plus kit, and barcoded samples were pooled and
547 sequenced on an Illumina HiSeq 2500 (single-end 100 bp reads). RNAseq data were analyzed
548 using the Geneious program (version 2023.0.4). Specifically, raw data were trimmed using BBDuk
549 with the following parameters: trim adapters (All Truseq), Kmer lengh 27, trim low quality on
550 both ends with minimum quality 30, discard short reads with minimum length 36 bp, minimum
551 entropy 0.1, entropy window size 4 and entropy Kmer size 5. Trimmed sequences were assembled
552 onto the CDC1551 genome (GenBank AE000516.2) using the Bowtie2 mapper[59] with end-to-end
553 alignment. Gene expression levels were then calculated and excluded ambiguously mapped reads
554 from calculation, with comparison of expression levels performed via DEseq2[60]. qRT-PCR
555 experiments were carried out and data analyzed as previously described[3].
556
557 **Macrophage culture and infections**
558 Bone marrow-derived macrophages were isolated from C57BL/6J wild type mice obtained from
559 Jackson Laboratories. The cells were cultured in DMEM supplemented with 10% FBS, 15% L-
560 cell conditioned media, 2 mM L-glutamine, 1 mM sodium pyruvate, and penicillin/streptomycin
561 when needed, and maintained in a 37˚C incubator with 5% CO_2. To induce the formation of foamy
562 macrophages, macrophages were pre-treated with macrophage medium supplemented with
563 oleate/albumin (0.42 mM sodium oleate, 0.35% BSA) complexes 24 hours prior to infection,
564 following a previously established protocol[35,36]. Macrophage infections with Mtb were carried out
565 as previously described[2,58]. For enumeration of colony forming units (CFUs), macrophages were

566 lysed using a solution of water containing 0.01% sodium dodecyl sulfate, and serial dilutions
567 plated on 7H10 agar plates supplemented with 100 µg/ml cycloheximide.
568
569 **Mouse Mtb infections**
570 C3HeB/FeJ wild type mice from Jackson Laboratories were intranasally infected with 10^3 CFUs
571 of Mtb in a volume of 35 µl, while under light anesthesia with 2% isoflurane[9,11,20]. Following
572 sacrifice using CO_2 at 2 or 6 weeks post-infection, the left lobe and accessory right lobe of the
573 lungs were homogenized in PBS containing 0.05% Tween 80. Serial dilutions of the homogenates
574 were plated on 7H10 agar plates supplemented with 100 µg/ml cycloheximide for the
575 quantification of CFUs.
576
577 **Confocal immunofluorescence microscopy**
578 Fixed murine lung lobes were processed and stained as previously described[9,61]. DAPI was used
579 at 1:500 (Invitrogen), Bodipy 493/503 was used at 1:500 (Invitrogen), and Alexa Fluor 647
580 phalloidin was used at 1:50 (Invitrogen). Imaging was performed on a Leica SP8 spectral confocal
581 microscope with 0.5 µm z-steps, and images reconstructed into 3-dimensions with Volocity
582 software (Quorum Technologies).
583
584 **Quantification and statistical analysis**
585 GraphPad Prism was used for all statistical analyses. Details of statistical tests performed are
586 indicated in the figure legends. $p<0.05$ was considered significant.
587
588 **SUPPORTING INFORMATION FIGURE AND TABLE LEGENDS**

589 **Figure S1. PhoPR deletion dampens Mtb response to acidic pH and Cl^-, in the absence or**
590 **presence of cholesterol**. Log-phase WT, Δ*phoPR*, and *phoPR** (complemented strain) Mtb were
591 exposed for 4 hours to (A) 7H9 or cholesterol media at pH 5.7, or (B) 7H9 or cholesterol media at
592 pH 7 + 250 mM NaCl, along with 7H9, pH 7 as the control condition. Fold change is as compared
593 to the 7H9, pH 7 condition in all cases. *sigA* was used as the control gene, and data are shown as
594 means ± SD from 3 technical replicates, representative of 3 experiments. p-values were obtained
595 with an unpaired t-test with Welch's correction and Holm-Sidak multiple comparisons, N.S. not
596 significant, * $p<0.05$, *** $p<0.001$, **** $p<0.0001$.
597
598 **Table S1. Results of CDC1551(*rv2390c'*::luciferase) transcription factor overexpression**
599 **pH/K^+ screen.**
600
601 **Table S2. Comparison of effect of acidic pH on genes differentially expressed ≥1 log_2-fold in**
602 **cholesterol in WT Mtb, after 4 hours exposure to cholesterol media at pH 5.7 or pH 7.**
603
604 **Table S3. Comparison of effect of cholesterol on genes differentially expressed ≥1 log_2-fold**
605 **in acidic pH in WT Mtb, after 4 hours exposure to cholesterol, pH 5.7 or 7H9, pH 5.7 media.**
606
607 **Table S4. Comparison of effect of *mce3R* deletion on genes differentially expressed ≥1 log_2-**
608 **fold in acidic pH in WT Mtb, after 4 hours exposure to 7H9, pH 5.7 medium.**
609
610 **Table S5. Comparison of effect of *mce3R* deletion on genes differentially expressed ≥1 log_2-**
611 **fold in cholesterol in WT Mtb, after 4 hours exposure to cholesterol, pH 7 medium.**

612

613 **Table S6. Comparison of effect of *mce3R* deletion on genes differentially expressed ≥1 log_2-**

614 **fold in cholesterol, pH 5.7 in WT Mtb, after 4 hours exposure to cholesterol, pH 5.7 medium.**

615

616 **REFERENCES**

617 1. Rohde, K.H., Abramovitch, R.B., and Russell, D.G. (2007). *Mycobacterium tuberculosis*

618 invasion of macrophages: linking bacterial gene expression to environmental cues. Cell Host

619 Microbe *2*, 352-364. 10.1016/j.chom.2007.09.006.

620 2. Tan, S., Sukumar, N., Abramovitch, R.B., Parish, T., and Russell, D.G. (2013).

621 *Mycobacterium tuberculosis* responds to chloride and pH as synergistic cues to the immune

622 status of its host cell. PLoS Pathog *9*, e1003282. 10.1371/journal.ppat.1003282.

623 3. MacGilvary, N.J., Kevorkian, Y.L., and Tan, S. (2019). Potassium response and homeostasis

624 in *Mycobacterium tuberculosis* modulates environmental adaptation and is important for host

625 colonization. PLoS Pathog *15*, e1007591. 10.1371/journal.ppat.1007591.

626 4. World Health Organization. (2022). Global tuberculosis report.

627 https://www.who.int/publications/i/item/9789240061729. (Last accessed 18 August 2023.)

628 5. Pérez, E., Samper, S., Bordas, Y., Guilhot, C., Gicquel, B., and Martín, C. (2001). An essential

629 role for *phoP* in *Mycobacterium tuberculosis* virulence. Mol Microbiol *41*, 179-187.

630 10.1046/j.1365-2958.2001.02500.x.

631 6. Walters, S.B., Dubnau, E., Kolesnikova, I., Laval, F., Daffe, M., and Smith, I. (2006). The

632 *Mycobacterium tuberculosis* PhoPR two-component system regulates genes essential for

633 virulence and complex lipid biosynthesis. Mol Microbiol *60*, 312-330. 10.1111/j.1365-

634 2958.2006.05102.x.

635 7. Arbues, A., Aguilo, J.I., Gonzalo-Asensio, J., Marinova, D., Uranga, S., Puentes, E.,
636 Fernandez, C., Parra, A., Cardona, P.J., Vilaplana, C., et al. (2013). Construction,
637 characterization and preclinical evaluation of MTBVAC, the first live-attenuated *M.*
638 *tuberculosis*-based vaccine to enter clinical trials. Vaccine *31*, 4867-4873.
639 10.1016/j.vaccine.2013.07.051.
640 8. Cardona, P.J., Asensio, J.G., Arbués, A., Otal, I., Lafoz, C., Gil, O., Caceres, N., Ausina, V.,
641 Gicquel, B., and Martin, C. (2009). Extended safety studies of the attenuated live tuberculosis
642 vaccine SO2 based on *phoP* mutant. Vaccine *27*, 2499-2505. 10.1016/j.vaccine.2009.02.060.
643 9. Lavin, R.C., and Tan, S. (2022). Spatial relationships of intra-lesion heterogeneity in
644 *Mycobacterium tuberculosis* microenvironment, replication status, and drug efficacy. PLoS
645 Pathog *18*, e1010459. 10.1371/journal.ppat.1010459.
646 10. Kumar, A., Toledo, J.C., Patel, R.P., Lancaster, J.R., Jr., and Steyn, A.J. (2007).
647 *Mycobacterium tuberculosis* DosS is a redox sensor and DosT is a hypoxia sensor. Proc Natl
648 Acad Sci USA *104*, 11568-11573. 10.1073/pnas.0705054104.
649 11. Giacalone, D., Yap, R.E., Ecker, A.M.V., and Tan, S. (2022). PrrA modulates *Mycobacterium*
650 *tuberculosis* response to multiple environmental cues and is critically regulated by
651 serine/threonine protein kinases. PLoS Genet *18*, e1010331. 10.1371/journal.pgen.1010331.
652 12. Haydel, S.E., Malhotra, V., Cornelison, G.L., and Clark-Curtiss, J.E. (2012). The *prrAB* two-
653 component system is essential for *Mycobacterium tuberculosis* viability and is induced under
654 nitrogen-limiting conditions. J Bacteriol *194*, 354-361. 10.1128/jb.06258-11.
655 13. Converse, P.J., Karakousis, P.C., Klinkenberg, L.G., Kesavan, A.K., Ly, L.H., Allen, S.S.,
656 Grosset, J.H., Jain, S.K., Lamichhane, G., Manabe, Y.C., et al. (2009). Role of the *dosR-dosS*

657 two-component regulatory system in *Mycobacterium tuberculosis* virulence in three animal
658 models. Infect Immun *77*, 1230-1237. 10.1128/iai.01117-08.
659 14. Mehra, S., Foreman, T.W., Didier, P.J., Ahsan, M.H., Hudock, T.A., Kissee, R., Golden, N.A.,
660 Gautam, U.S., Johnson, A.M., Alvarez, X., et al. (2015). The DosR regulon modulates
661 adaptive immunity and is essential for *Mycobacterium tuberculosis* persistence. Am J Respir
662 Crit Care Med *191*, 1185-1196. 10.1164/rccm.201408-1502OC.
663 15. Gautam, U.S., McGillivray, A., Mehra, S., Didier, P.J., Midkiff, C.C., Kissee, R.S., Golden,
664 N.A., Alvarez, X., Niu, T., Rengarajan, J., et al. (2015). DosS Is required for the complete
665 virulence of *Mycobacterium tuberculosis* in mice with classical granulomatous lesions. Am J
666 Respir Cell Mol Biol *52*, 708-716. 10.1165/rcmb.2014-0230OC.
667 16. Pandey, A.K., and Sassetti, C.M. (2008). Mycobacterial persistence requires the utilization of
668 host cholesterol. Proc Natl Acad Sci USA *105*, 4376-4380. 10.1073/pnas.0711159105.
669 17. Nesbitt, N.M., Yang, X., Fontán, P., Kolesnikova, I., Smith, I., Sampson, N.S., and Dubnau,
670 E. (2010). A thiolase of *Mycobacterium tuberculosis* is required for virulence and production
671 of androstenedione and androstadienedione from cholesterol. Infect Immun *78*, 275-282.
672 10.1128/iai.00893-09.
673 18. Gouzy, A., Healy, C., Black, K.A., Rhee, K.Y., and Ehrt, S. (2021). Growth of
674 *Mycobacterium tuberculosis* at acidic pH depends on lipid assimilation and is accompanied
675 by reduced GAPDH activity. Proc Natl Acad Sci USA *118*. 10.1073/pnas.2024571118.
676 19. Baker, J.J., Johnson, B.K., and Abramovitch, R.B. (2014). Slow growth of *Mycobacterium*
677 *tuberculosis* at acidic pH is regulated by *phoPR* and host-associated carbon sources. Mol
678 Microbiol *94*, 56-69. 10.1111/mmi.12688.

679 20. Lavin, R.C., Johnson, C., Ahn, Y.M., Kremiller, K.M., Sherwood, M., Patel, J.S., Pan, Y.,
680 Russo, R., MacGilvary, N.J., Giacalone, D., et al. (2021). Targeting *Mycobacterium*
681 *tuberculosis* response to environmental cues for the development of effective antitubercular
682 drugs. PLoS Biol *19*, e3001355. 10.1371/journal.pbio.3001355.
683 21. Theriault, M.E., Pisu, D., Wilburn, K.M., Lê-Bury, G., MacNamara, C.W., Michael Petrassi,
684 H., Love, M., Rock, J.M., VanderVen, B.C., and Russell, D.G. (2022). Iron limitation in *M.*
685 *tuberculosis* has broad impact on central carbon metabolism. Commun Biol *5*, 685.
686 10.1038/s42003-022-03650-z.
687 22. Kurthkoti, K., Amin, H., Marakalala, M.J., Ghanny, S., Subbian, S., Sakatos, A., Livny, J.,
688 Fortune, S.M., Berney, M., and Rodriguez, G.M. (2017). The capacity of *Mycobacterium*
689 *tuberculosis* to survive iron starvation might enable it to persist in iron-deprived
690 microenvironments of human granulomas. mBio *8*, e01092-17. 10.1128/mBio.01092-17.
691 23. Casali, N., White, A.M., and Riley, L.W. (2006). Regulation of the *Mycobacterium*
692 *tuberculosis mce1* operon. J Bacteriol *188*, 441-449. 10.1128/jb.188.2.441-449.2006.
693 24. Nazarova, E.V., Montague, C.R., La, T., Wilburn, K.M., Sukumar, N., Lee, W., Caldwell, S.,
694 Russell, D.G., and VanderVen, B.C. (2017). Rv3723/LucA coordinates fatty acid and
695 cholesterol uptake in *Mycobacterium tuberculosis*. Elife *6*, e26969. 10.7554/eLife.26969.
696 25. Yousuf, S., Angara, R.K., Roy, A., Gupta, S.K., Misra, R., and Ranjan, A. (2018).
697 Mce2R/Rv0586 of *Mycobacterium tuberculosis* is the functional homologue of FadR(*E. coli*).
698 Microbiology *164*, 1133-1145. 10.1099/mic.0.000686.
699 26. Delmar, J.A., Chou, T.H., Wright, C.C., Licon, M.H., Doh, J.K., Radhakrishnan, A., Kumar,
700 N., Lei, H.T., Bolla, J.R., Rajashankar, K.R., et al. (2015). Structural basis for the regulation

701 of the MmpL transporters of *Mycobacterium tuberculosis*. J Biol Chem *290*, 28559-28574.
702 10.1074/jbc.M115.683797.
703 27. Turapov, O., Waddell, S.J., Burke, B., Glenn, S., Sarybaeva, A.A., Tudo, G., Labesse, G.,
704 Young, D.I., Young, M., Andrew, P.W., et al. (2014). Oleoyl coenzyme A regulates
705 interaction of transcriptional regulator RaaS (Rv1219c) with DNA in mycobacteria. J Biol
706 Chem *289*, 25241-25249. 10.1074/jbc.M114.577338.
707 28. Kendall, S.L., Withers, M., Soffair, C.N., Moreland, N.J., Gurcha, S., Sidders, B., Frita, R.,
708 Ten Bokum, A., Besra, G.S., Lott, J.S., and Stoker, N.G. (2007). A highly conserved
709 transcriptional repressor controls a large regulon involved in lipid degradation in
710 *Mycobacterium smegmatis* and *Mycobacterium tuberculosis*. Mol Microbiol *65*, 684-699.
711 10.1111/j.1365-2958.2007.05827.x.
712 29. Kendall, S.L., Burgess, P., Balhana, R., Withers, M., Ten Bokum, A., Lott, J.S., Gao, C.,
713 Uhia-Castro, I., and Stoker, N.G. (2010). Cholesterol utilization in mycobacteria is controlled
714 by two TetR-type transcriptional regulators: *kstR* and *kstR2*. Microbiology *156*, 1362-1371.
715 10.1099/mic.0.034538-0.
716 30. Griffin, J.E., Pandey, A.K., Gilmore, S.A., Mizrahi, V., McKinney, J.D., Bertozzi, C.R., and
717 Sassetti, C.M. (2012). Cholesterol catabolism by *Mycobacterium tuberculosis* requires
718 transcriptional and metabolic adaptations. Chem Biol *19*, 218-227.
719 10.1016/j.chembiol.2011.12.016.
720 31. Santangelo, M.P., Klepp, L., Nuñez-García, J., Blanco, F.C., Soria, M., García-Pelayo,
721 M.D.C., Bianco, M.V., Cataldi, A.A., Golby, P., Jackson, M., et al. (2009). Mce3R, a TetR-
722 type transcriptional repressor, controls the expression of a regulon involved in lipid

723 metabolism in *Mycobacterium tuberculosis*. Microbiology *155*, 2245-2255.
724 10.1099/mic.0.027086-0.
725 32. Santangelo, M.A.P., Goldstein, J., Alito, A., Gioffré, A., Caimi, K., Zabal, O., Zumárraga,
726 M.N., Romano, M.I., Cataldi, A.A., and Bigi, F. (2002). Negative transcriptional regulation
727 of the *mce3* operon in *Mycobacterium tuberculosis*. Microbiology *148*, 2997-3006.
728 10.1099/00221287-148-10-2997.
729 33. Santangelo, M.P., Blanco, F.C., Bianco, M.V., Klepp, L.I., Zabal, O., Cataldi, A.A., and Bigi,
730 F. (2008). Study of the role of Mce3R on the transcription of *mce* genes of *Mycobacterium*
731 *tuberculosis*. BMC Microbiol *8*, 38. 10.1186/1471-2180-8-38.
732 34. Wilburn, K.M., Fieweger, R.A., and VanderVen, B.C. (2018). Cholesterol and fatty acids
733 grease the wheels of *Mycobacterium tuberculosis* pathogenesis. Pathog Dis *76*, fty021.
734 10.1093/femspd/fty021.
735 35. Listenberger, L.L., and Brown, D.A. (2007). Fluorescent detection of lipid droplets and
736 associated proteins. Curr Protoc Cell Biol *Chapter 24*, Unit 24.22.
737 10.1002/0471143030.cb2402s35.
738 36. Podinovskaia, M., Lee, W., Caldwell, S., and Russell, D.G. (2013). Infection of macrophages
739 with *Mycobacterium tuberculosis* induces global modifications to phagosomal function. Cell
740 Microbiol *15*, 843-859. 10.1111/cmi.12092.
741 37. Pethe, K., Swenson, D.L., Alonso, S., Anderson, J., Wang, C., and Russell, D.G. (2004).
742 Isolation of *Mycobacterium tuberculosis* mutants defective in the arrest of phagosome
743 maturation. Proc Natl Acad Sci USA *101*, 13642-13647. 10.1073/pnas.0401657101.
744 38. Driver, E.R., Ryan, G.J., Hoff, D.R., Irwin, S.M., Basaraba, R.J., Kramnik, I., and Lenaerts,
745 A.J. (2012). Evaluation of a mouse model of necrotic granuloma formation using C3HeB/FeJ

746 mice for testing of drugs against *Mycobacterium tuberculosis*. Antimicrob Agents Chemother
747 *56*, 3181-3195. 10.1128/aac.00217-12.
748 39. Irwin, S.M., Driver, E., Lyon, E., Schrupp, C., Ryan, G., Gonzalez-Juarrero, M., Basaraba,
749 R.J., Nuermberger, E.L., and Lenaerts, A.J. (2015). Presence of multiple lesion types with
750 vastly different microenvironments in C3HeB/FeJ mice following aerosol infection with
751 *Mycobacterium tuberculosis*. Dis Model Mech *8*, 591-602. 10.1242/dmm.019570.
752 40. Harper, J., Skerry, C., Davis, S.L., Tasneen, R., Weir, M., Kramnik, I., Bishai, W.R., Pomper,
753 M.G., Nuermberger, E.L., and Jain, S.K. (2012). Mouse model of necrotic tuberculosis
754 granulomas develops hypoxic lesions. J Infect Dis *205*, 595-602. 10.1093/infdis/jir786.
755 41. MacGilvary, N.J., and Tan, S. (2018). Fluorescent *Mycobacterium tuberculosis* reporters:
756 illuminating host-pathogen interactions. Pathog Dis *76*, fty017. 10.1093/femspd/fty017.
757 42. Peyron, P., Vaubourgeix, J., Poquet, Y., Levillain, F., Botanch, C., Bardou, F., Daffé, M.,
758 Emile, J.F., Marchou, B., Cardona, P.J., et al. (2008). Foamy macrophages from tuberculous
759 patients' granulomas constitute a nutrient-rich reservoir for *M. tuberculosis* persistence. PLoS
760 Pathog *4*, e1000204. 10.1371/journal.ppat.1000204.
761 43. Russell, D.G., Cardona, P.J., Kim, M.J., Allain, S., and Altare, F. (2009). Foamy macrophages
762 and the progression of the human tuberculosis granuloma. Nat Immunol *10*, 943-948.
763 10.1038/ni.1781.
764 44. Chen, Y., Quirk, N.F., and Tan, S. (2023). Shining a light on bacterial environmental cue
765 integration and its relation to metabolism. Mol Microbiol *120*, 71-74. 10.1111/mmi.15065.
766 45. Harper, L., Balasubramanian, D., Ohneck, E.A., Sause, W.E., Chapman, J., Mejia-Sosa, B.,
767 Lhakhang, T., Heguy, A., Tsirigos, A., Ueberheide, B., et al. (2018). *Staphylococcus aureus*

768 responds to the central metabolite pyruvate to regulate virulence. mBio *9*, e02272-17.
769 10.1128/mBio.02272-17.
770 46. Rosenberg, G., Yehezkel, D., Hoffman, D., Mattioli, C.C., Fremder, M., Ben-Arosh, H.,
771 Vainman, L., Nissani, N., Hen-Avivi, S., Brenner, S., et al. (2021). Host succinate is an
772 activation signal for *Salmonella* virulence during intracellular infection. Science *371*, 400-
773 405. 10.1126/science.aba8026.
774 47. Maity, D., Singh, D., and Bandhu, A. (2022). Mce1R of *Mycobacterium tuberculosis* prefers
775 long-chain fatty acids as specific ligands: a computational study. Mol Divers. Nov 16 (online
776 ahead of print). 10.1007/s11030-022-10566-7.
777 48. Pandey, M., Talwar, S., Pal, R., Nain, V., Johri, S., Singhal, A., and Pandey, A.K. (2023).
778 Transcription factor *mce3R* modulates antibiotics and disease persistence in *Mycobacterium*
779 *tuberculosis*. Res Microbiol, 104082. 10.1016/j.resmic.2023.104082.
780 49. Ehrt, S., and Schnappinger, D. (2009). Mycobacterial survival strategies in the phagosome:
781 defence against host stresses. Cell Microbiol *11*, 1170-1178. 10.1111/j.1462-
782 5822.2009.01335.x.
783 50. Stingl, K., Brandt, S., Uhlemann, E.M., Schmid, R., Altendorf, K., Zeilinger, C., Ecobichon,
784 C., Labigne, A., Bakker, E.P., and de Reuse, H. (2007). Channel-mediated potassium uptake
785 in *Helicobacter pylori* is essential for gastric colonization. EMBO J *26*, 232-241.
786 10.1038/sj.emboj.7601471.
787 51. Do, E.A., and Gries, C.M. (2021). Beyond homeostasis: Potassium and pathogenesis during
788 bacterial infections. Infect Immun *89*, e0076620. 10.1128/iai.00766-20.

789 52. Barbera, N., Ayee, M.A.A., Akpa, B.S., and Levitan, I. (2017). Differential effects of sterols
790 on ion channels: Stereospecific binding vs stereospecific response. Curr Top Membr *80*, 25-
791 50. 10.1016/bs.ctm.2017.06.001.
792 53. Rosenhouse-Dantsker, A., Noskov, S., Durdagi, S., Logothetis, D.E., and Levitan, I. (2013).
793 Identification of novel cholesterol-binding regions in Kir2 channels. J Biol Chem *288*, 31154-
794 31164. 10.1074/jbc.M113.496117.
795 54. Singh, D.K., Rosenhouse-Dantsker, A., Nichols, C.G., Enkvetchakul, D., and Levitan, I.
796 (2009). Direct regulation of prokaryotic Kir channel by cholesterol. J Biol Chem *284*, 30727-
797 30736. 10.1074/jbc.M109.011221.
798 55. Corradi, V., Bukiya, A.N., Miranda, W.E., Cui, M., Plant, L.D., Logothetis, D.E., Tieleman,
799 D.P., Noskov, S.Y., and Rosenhouse-Dantsker, A. (2022). A molecular switch controls the
800 impact of cholesterol on a Kir channel. Proc Natl Acad Sci USA *119*, e2109431119.
801 10.1073/pnas.2109431119.
802 56. Cholo, M.C., Boshoff, H.I., Steel, H.C., Cockeran, R., Matlola, N.M., Downing, K.J.,
803 Mizrahi, V., and Anderson, R. (2006). Effects of clofazimine on potassium uptake by a Trk-
804 deletion mutant of *Mycobacterium tuberculosis*. J Antimicrob Chemother *57*, 79-84.
805 10.1093/jac/dki409.
806 57. Yang, X., Yuan, T., Ma, R., Chacko, K.I., Smith, M., Deikus, G., Sebra, R., Kasarskis, A.,
807 van Bakel, H., Franzblau, S.G., and Sampson, N.S. (2019). Mce3R stress-resistance pathway
808 is vulnerable to small-molecule targeting that improves tuberculosis drug activities. ACS
809 Infect Dis *5*, 1239-1251. 10.1021/acsinfecdis.9b00099.

810 58. Abramovitch, R.B., Rohde, K.H., Hsu, F.F., and Russell, D.G. (2011). *aprABC*: a
811 *Mycobacterium tuberculosis* complex-specific locus that modulates pH-driven adaptation to
812 the macrophage phagosome. Mol Microbiol *80*, 678-694. 10.1111/j.1365-2958.2011.07601.x.
813 59. Langmead, B., and Salzberg, S.L. (2012). Fast gapped-read alignment with Bowtie 2. Nat
814 Methods *9*, 357-359. 10.1038/nmeth.1923.
815 60. Love, M.I., Huber, W., and Anders, S. (2014). Moderated estimation of fold change and
816 dispersion for RNA-seq data with DESeq2. Genome Biol *15*, 550. 10.1186/s13059-014-0550-
817 8.
818 61. Giacalone, D., Huang, L., and Tan, S. (2021). Exploiting fluorescent proteins to understand
819 *Mycobacterium tuberculosis* biology. Methods Mol Biol *2314*, 365-383. 10.1007/978-1-
820 0716-1460-0_17.
821

Figure 1

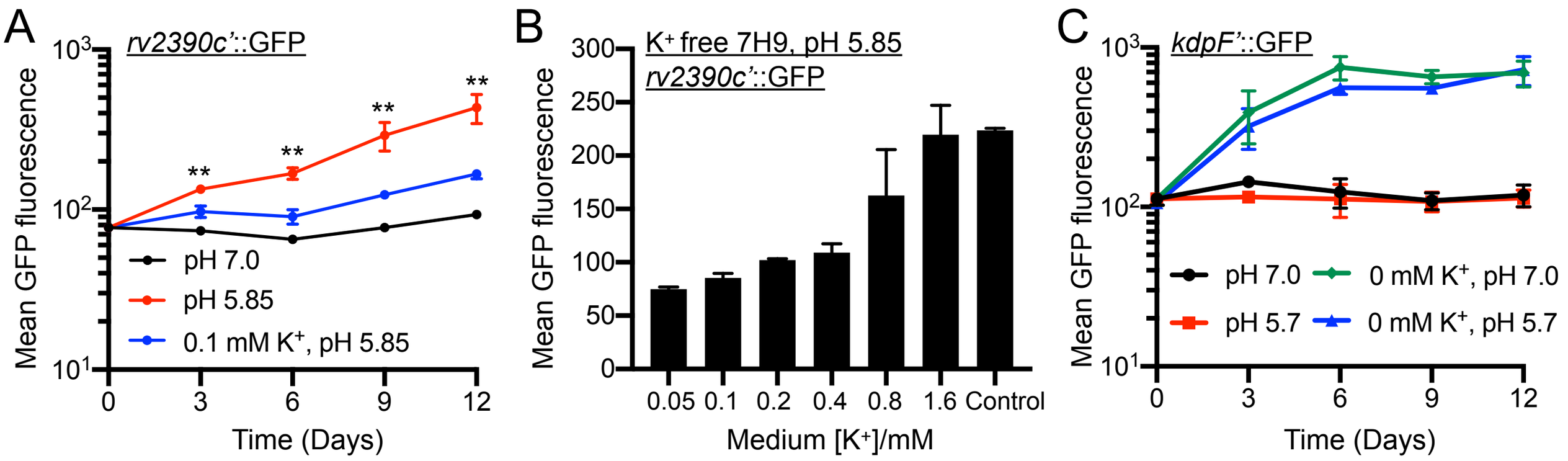

Figure 1. Environmental K^+ levels modulate Mtb transcriptional response to acidic pH. (A) *rv2390c'*::GFP reporter response to acidic pH is dampened in the presence of low [K^+]. Mtb(*rv2390c'*::GFP) was grown in 7H9, pH 7.0 or pH 5.85 media, or in K^+-free 7H9, pH 5.85 medium, supplemented with 0.1 mM K^+. Samples were taken at indicated time points, fixed, and GFP induction analyzed by flow cytometry. Data are shown as means ± SD from 3 experiments. p-values were obtained with an unpaired t-test with Welch's correction, and compare the 7H9, pH 5.85 to the 0.1 mM K^+, pH 5.85 condition. ** $p<0.01$. (B) Dampening of Mtb response to acidic pH by low K^+ is concentration dependent. Mtb(*rv2390c'*::GFP) was grown in 7H9, pH 5.85 medium ("control"), or in K^+-free 7H9, pH 5.85 medium, supplemented with indicated amounts of K^+. Samples were taken 9 days post-assay start, fixed, and GFP induction analyzed by flow cytometry. Data are shown as means ± SD from 3 experiments. (C) Mtb response to low [K^+] is not affected by environmental pH. Mtb(*kdpF'*::GFP) was grown in 7H9, pH 7.0 or pH 5.7, or in K^+-free 7H9, pH 7 or pH 5.7 media. Samples were taken at indicated time points, fixed, and GFP induction analyzed by flow cytometry. Data are shown as means ± SD from 3 experiments.

Figure 2

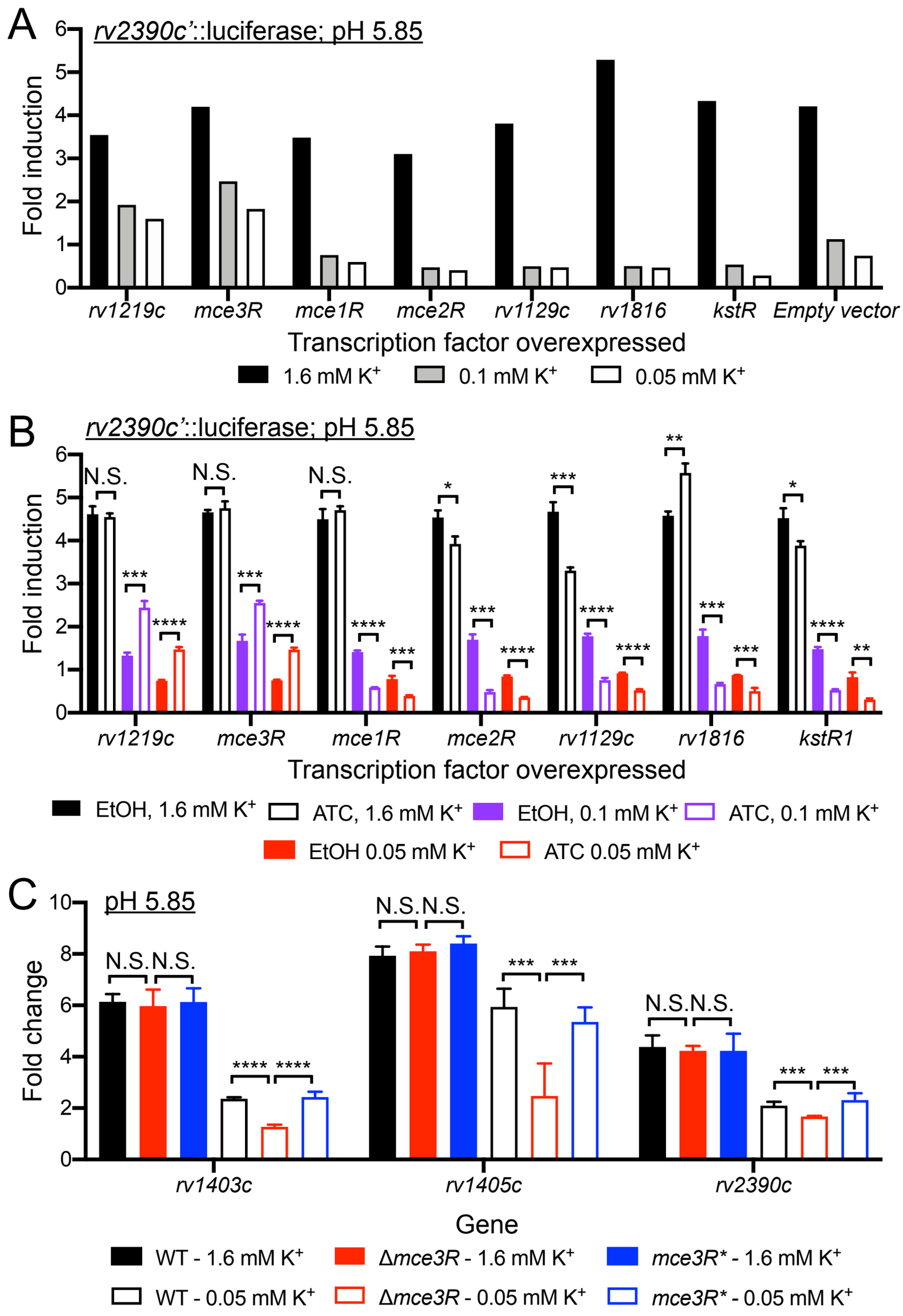

Figure 2. A *rv2390c*'::luciferase reporter transcription factor overexpression screen identifies lipid utilization regulators as modulators of the interplay between environmental [K^+] and Mtb pH response. (A and B) Lipid utilization regulator hits from reporter-based, inducible transcription factor (TF) overexpression screen. A library of inducible TF overexpression plasmids (P_1'::*TF*-FLAG-tetON) in the background of a Mtb(*rv2390c*'::luciferase) strain was screened for their response to acidic pH in the presence of low [K^+]. TF overexpression was induced by adding 200 ng/ml of anhydrotetracycline (ATC) 1 day before Mtb was exposed to K^+-free 7H9, pH 7 or K^+-free 7H9, pH 5.85 media supplemented with 1.6 mM or 0.05 mM K^+. 9 days post-exposure (continuous ATC presence), light output (relative light units, RLU) and OD_{600} were measured. Fold induction compares RLU/OD_{600} in each condition to RLU/OD_{600} in the control K^+-free 7H9, pH 7 condition. (A) shows results of the lipid utilization regulator hits, together with an empty vector plasmid control. (B) shows validation of the screen hits in (A), with each hit TF compared to its uninduced control (ethanol, "EtOH", as a carrier control). In (B), data are shown as means ± SD from three experiments, and p-values were obtained with an unpaired t-test with Welch's correction. N.S. not significant, * $p<0.05$, ** $p<0.01$, *** $p<0.001$, **** $p<0.0001$. (C) Mce3R modulates the interplay between environmental [K^+] and Mtb pH response. Log-phase WT, Δ*mce3R* and *mce3R** (complemented mutant) were exposed for 4 hours to K^+-free 7H9, pH 7 or K^+-free 7H9, pH 5.85 media supplemented with 1.6 mM or 0.05 mM K^+, before RNA was extracted for qRT-PCR analysis. Fold change is as compared to the K^+-free 7H9, pH 7 condition. *sigA* was used as the control gene, and data are shown as means ± SD from 3 technical replicates, representative of 3 experiments. p-values were obtained with an unpaired t-test with Welch's correction and Holm-Sidak multiple comparisons, N.S. not significant, *** $p<0.001$, **** $p<0.0001$.

Figure 3

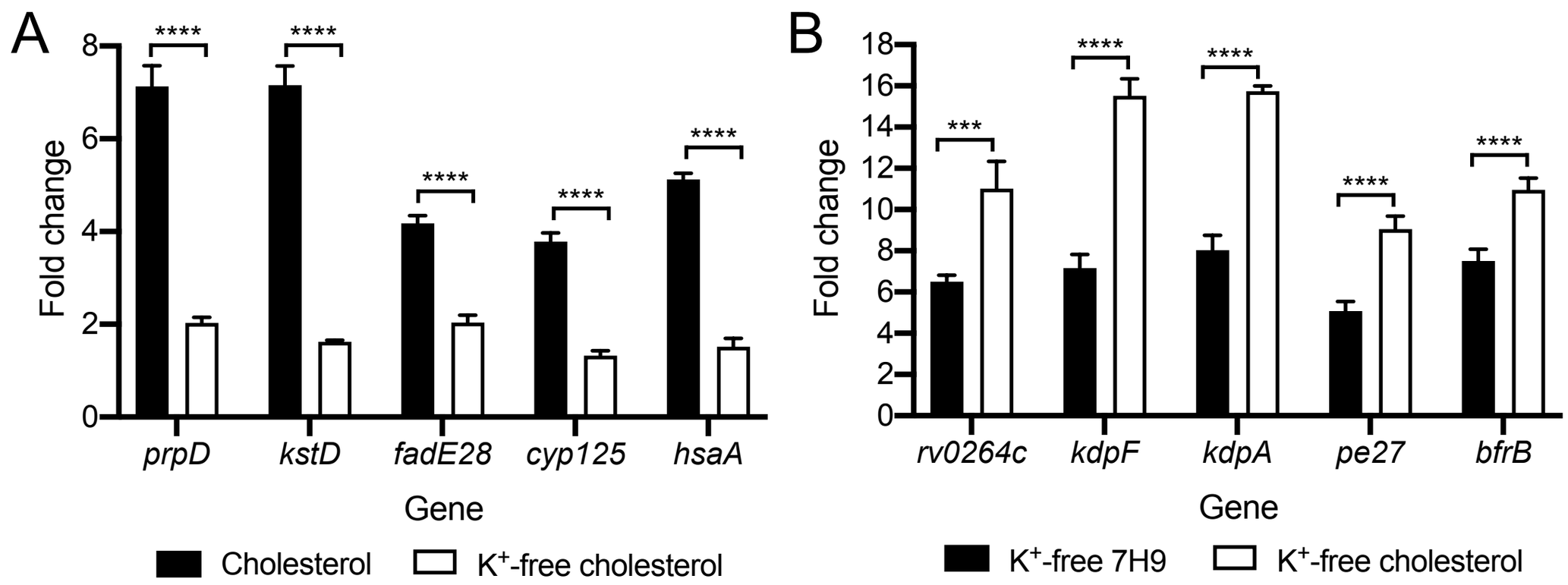

Figure 3. Mtb transcriptional response to low [K$^+$] and cholesterol are linked. (A) Low [K$^+$] dampens Mtb response to cholesterol. Log-phase Mtb was exposed for 4 hours to (i) 7H9, pH 7, (ii) cholesterol, pH 7, or (iii) K$^+$-free cholesterol, pH 7 media, before RNA was extracted for qRT-PCR analysis. (B) Cholesterol augments Mtb response to low [K$^+$]. Log-phase Mtb was exposed for 4 hours to (i) 7H9, pH 7, (ii) K$^+$-free 7H9, pH 7, or (iii) K$^+$-free cholesterol, pH 7 media, before RNA was extracted for qRT-PCR analysis. Fold change is as compared to the 7H9, pH 7 condition in all cases. *sigA* was used as the control gene, and data are shown as means ± SD from 3 technical replicates, representative of 3 experiments. p-values were obtained with an unpaired t-test with Welch's correction, *** $p<0.001$, **** $p<0.0001$.

Figure 4

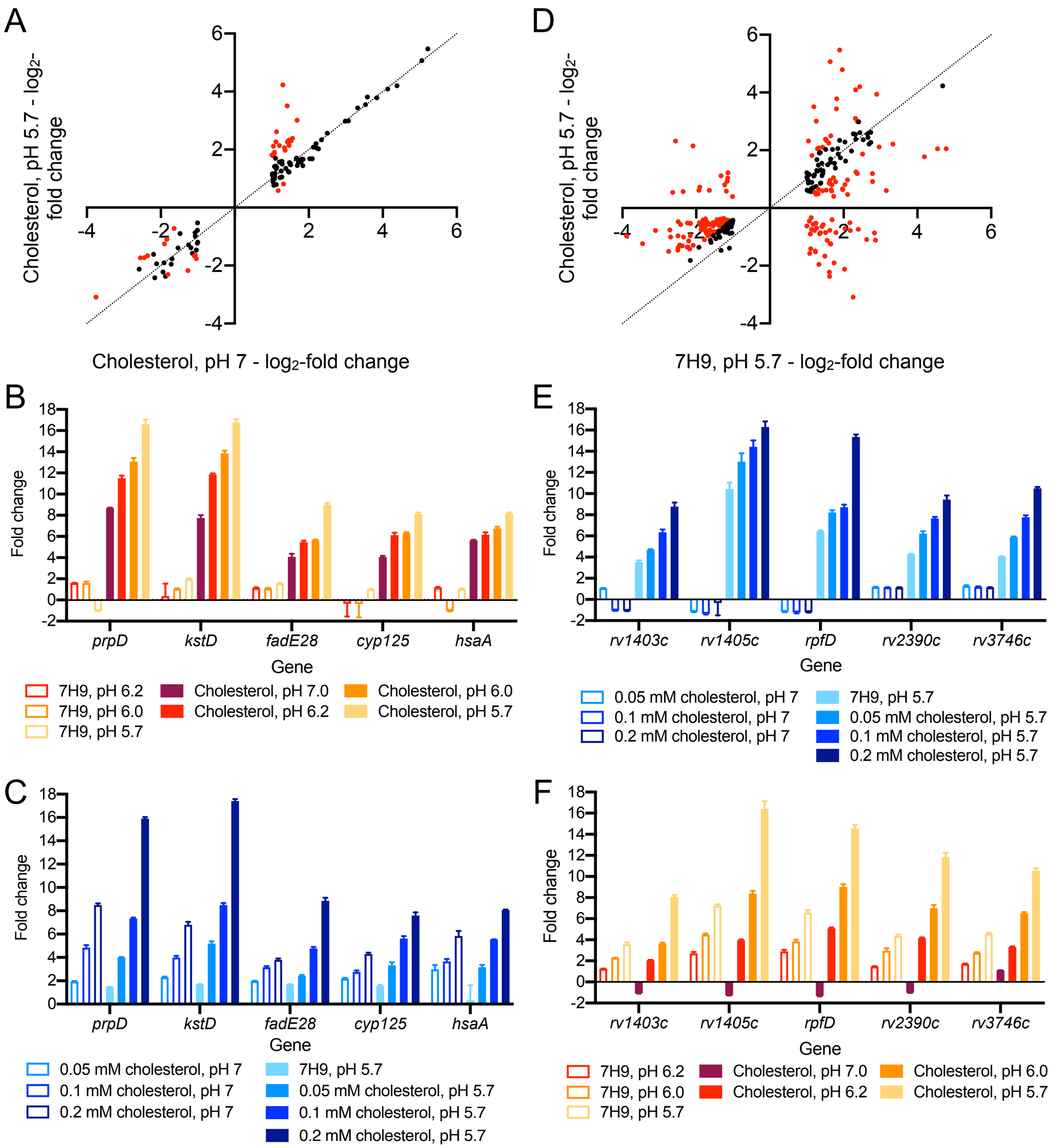
A
Cholesterol, pH 5.7 - log2-fold change
Cholesterol, pH 7 - log2-fold change
D
Cholesterol, pH 5.7 - log2-fold change
7H9, pH 5.7 - log2-fold change
B
Fold change
prpD
kstD
fadE28
cyp125
hsaA
Gene
7H9, pH 6.2
7H9, pH 6.0
7H9, pH 5.7
Cholesterol, pH 7.0
Cholesterol, pH 6.2
Cholesterol, pH 6.0
Cholesterol, pH 5.7
E
Fold change
rv1403c
rv1405c
rpfD
rv2390c
rv3746c
Gene
0.05 mM cholesterol, pH 7
0.1 mM cholesterol, pH 7
0.2 mM cholesterol, pH 7
7H9, pH 5.7
0.05 mM cholesterol, pH 5.7
0.1 mM cholesterol, pH 5.7
0.2 mM cholesterol, pH 5.7
C
Fold change
prpD
kstD
fadE28
cyp125
hsaA
Gene
0.05 mM cholesterol, pH 7
0.1 mM cholesterol, pH 7
0.2 mM cholesterol, pH 7
7H9, pH 5.7
0.05 mM cholesterol, pH 5.7
0.1 mM cholesterol, pH 5.7
0.2 mM cholesterol, pH 5.7
F
Fold change
rv1403c
rv1405c
rpfD
rv2390c
rv3746c
Gene
7H9, pH 6.2
7H9, pH 6.0
7H9, pH 5.7
Cholesterol, pH 7.0
Cholesterol, pH 6.2
Cholesterol, pH 6.0
Cholesterol, pH 5.7

Figure 4. Mtb transcriptional response to acidic pH and cholesterol are linked globally. (A and D) Global changes in Mtb response to cholesterol and acidic pH in the simultaneous presence of both signals. Log-phase Mtb was exposed for 4 hours to (i) 7H9, pH 7, (ii) 7H9, pH 5.7, (iii) cholesterol, pH 7, or (iv) cholesterol, pH 5.7 media, before RNA was extracted for RNAseq analysis. Log_2-fold change compares gene expression in each indicated condition to the 7H9, pH 7 condition. Genes marked in red had a log_2-fold change ≥ 0.6 between the two conditions compared ($p<0.05$, FDR<0.01 in both sets, with log_2-fold change ≥ 1 in the single condition set). (B and C) Effect of acidic pH on Mtb response to cholesterol is concentration dependent. Log-phase Mtb was exposed to the indicated conditions, along with control 7H9, pH7 condition, for 4 hours, before RNA was extracted for qRT-PCR analysis. (E and F) Effect of cholesterol on Mtb response to acidic pH is concentration dependent. For all qRT-PCR data, fold change is as compared to the 7H9, pH 7 condition, and data are shown as means ± SD from 3 technical replicates, representative of 3 experiments.

Figure 5

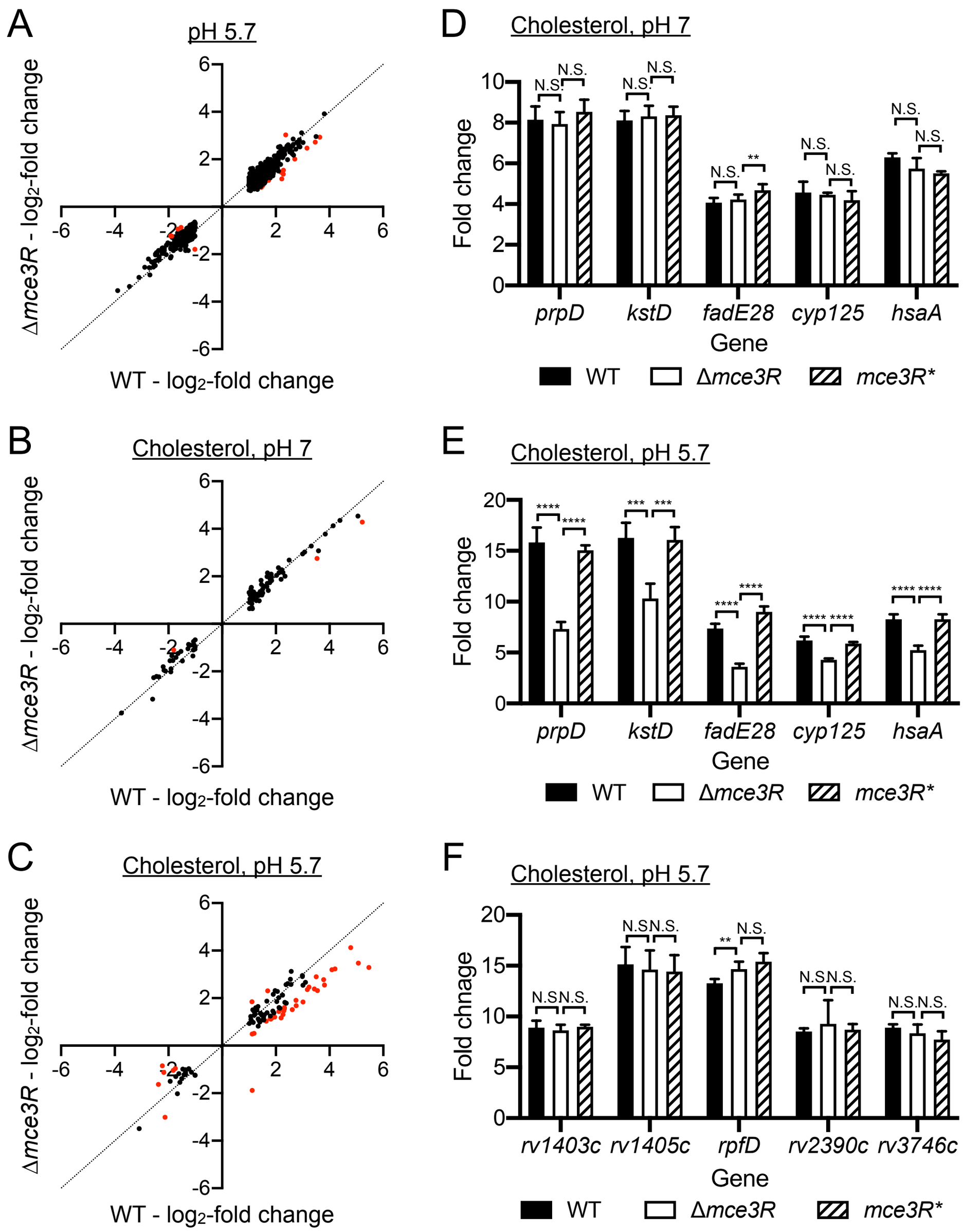

Figure 5. Mce3R regulates Mtb response to cholesterol only in the context of acidic pH. Log-phase WT, Δ*mce3R* and *mce3R** (complemented strain) Mtb were exposed for 4 hours to (i) 7H9, pH 7, (ii) 7H9, pH 5.7, (iii) cholesterol, pH 7, or (iv) cholesterol, pH 5.7 media, before RNA was extracted for RNAseq (A-C) or qRT-PCR (D-F). For RNAseq data, $\log_2$-fold change compares gene expression in each indicated condition to the 7H9, pH 7 condition. Genes marked in red had a $\log_2$-fold change ≥ 0.6 between Δ*mce3R* and WT strains in the indicated condition ($p<0.05$, FDR<0.01 in both sets, with $\log_2$-fold change ≥1 in WT). For qRT-PCR data, fold change is as compared to the 7H9, pH 7 condition. Data are shown as means ± SD from 3 technical replicates, representative of 3 independent experiments. p-values were obtained with as unpaired t-test with Welch's correction and Holm-Sidak multiple comparisons. N.S. not significant, ** $p<0.01$, *** $p<0.001$, **** $p<0.0001$.

Figure 6

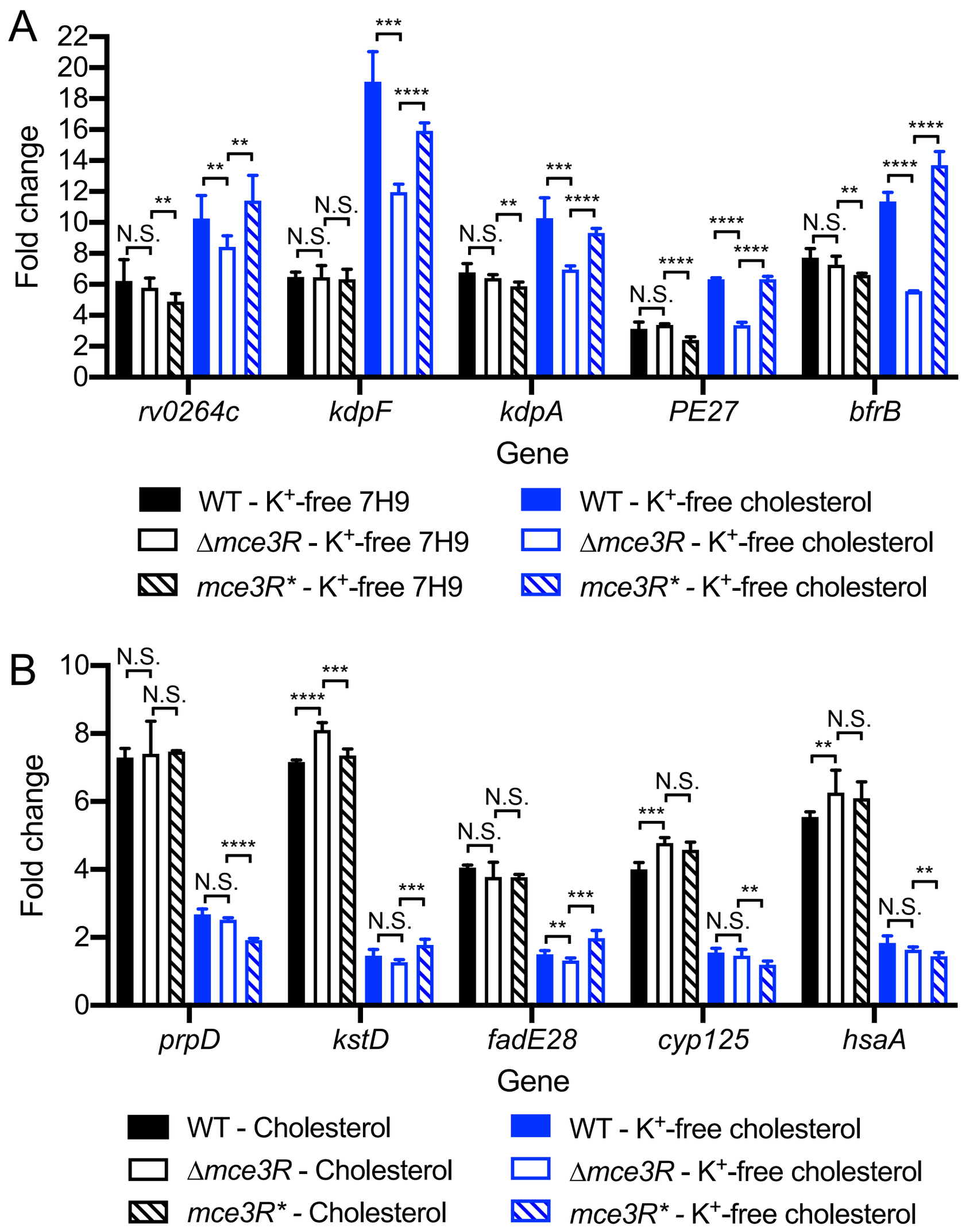

Figure 6. Mce3R deletion dampens Mtb response to K^+ in the presence of cholesterol. Log-phase WT, Δ*mce3R*, and *mce3R** (complemented strain) Mtb were exposed for 4 hours to (A) K^+-free 7H9 or cholesterol media at pH 7, or (B) cholesterol or K^+-free cholesterol media at pH 7, along with 7H9, pH 7 as the control condition. Fold change is as compared to the 7H9, pH 7 condition in all cases. *sigA* was used as the control gene, and data are shown as means ± SD from 3 technical replicates, representative of 3 experiments. p-values were obtained with an unpaired t-test with Welch's correction and Holm-Sidak multiple comparisons, N.S. not significant, ** $p<0.01$, *** $p<0.001$, **** $p<0.0001$.

Figure 7

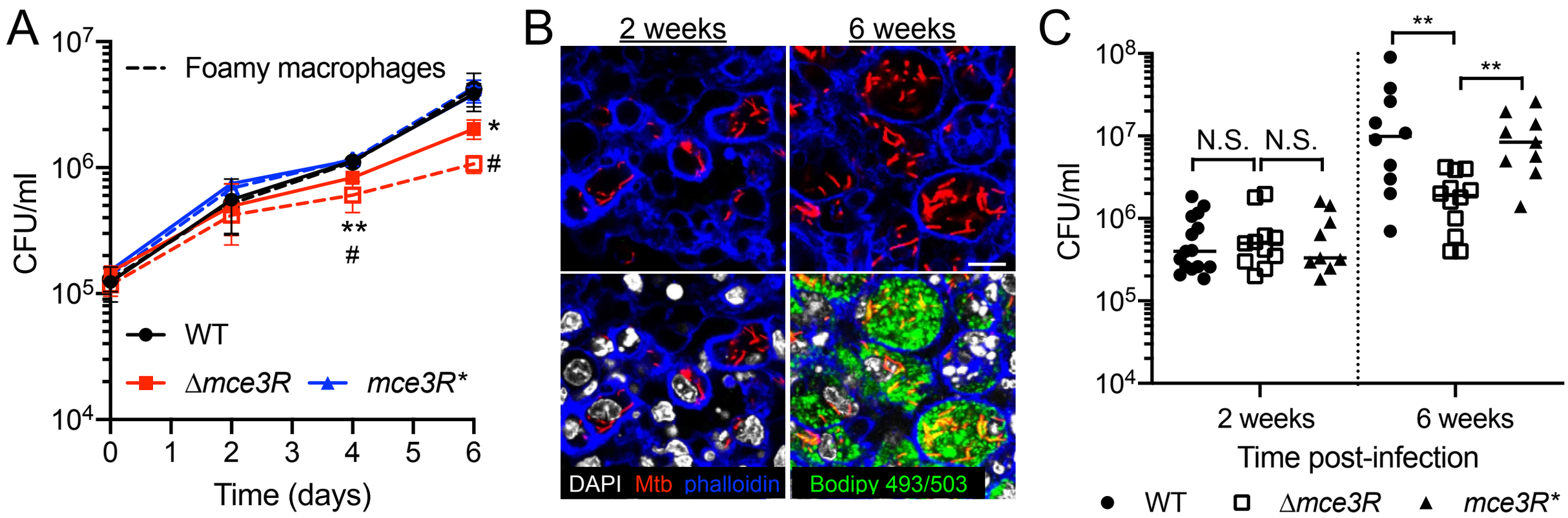

Figure 7. A Δ*mce3R* Mtb mutant is attenuated for host colonization in the presence of lipids. (A) Δ*mce3R* Mtb is attenuated for macrophage colonization. Murine bone marrow-derived macrophages untreated or pre-treated with oleate for 24 hours to induce foamy macrophages were infected with WT, Δ*mce3R*, or *mce3R** (complemented mutant) Mtb, and colony forming units (CFUs) tracked over time. Data are shown as means ± SD from 3 wells, representative of 3 independent experiments. p-values were obtained with an unpaired t-test with Welch's correction, comparing Δ*mce3R* to WT Mtb in untreated macrophages (*) or foamy macrophages (#). */# $p<0.05$, ** $p<0.01$. (B) Mtb is present in foamy macrophages 6 weeks post-infection in C3HeB/FeJ mice. C3HeB/FeJ mice were infected with Mtb constitutively expressing mCherry, and animals sacrificed at 2 or 6 weeks post-infection. Lungs were fixed and processed for confocal microscopy imaging. Images shown are z-slices from reconstructed 3D images. Nuclei are shown in grayscale (DAPI), all bacteria are marked in red (mCherry), f-actin is shown in blue (phalloidin), and lipid droplets are shown in green (Bodipy 493/503). Scale bar 10 µm. (C) Δ*mce3R* Mtb is attenuated for colonization in a murine infection model. C3HeB/FeJ mice were infected with WT, Δ*mce3R*, or *mce3R** Mtb, and lung homogenates plated for CFUs 2 or 6 weeks post-infection. p-values were obtained with a Mann-Whitney statistical test. N.S. not significant, **$p<0.01$.